Feature-aware Manifold Meshing and Remeshing of Point Clouds and Polyhedral Surfaces with Guaranteed Smallest Edge Length

Supplementary Material

In this supplementary material, we present a pseudo code segment summarizing Sections 3.3 to 3.7 and results of the algorithm introduced in our submission, applied to the complete set of twenty models as provided by the authors of [1]. See Figure 1 for all models. In order to emphasize the overall simple structure and to allow for easy reproduction of the algorithm presented here, we provide the following pseudo code fragment.

Algorithm 1 Isotropic Point Cloud Meshing using unit Spheres

Input: point cloud $\mathcal{P}$, normal field $\mathcal{N}$, target edge length d, splat size s, starting vertices q, q', window size w, maximum border length $\partial_{\max}$
Output: triangle mesh $\mathcal{T}$ with edge lengths close to uniformity

Build box grid, register splats in all boxes up to distance d (possibly with individual splat sizes), filter points according to the average normal, compute box normals.
Project q and q' to their closest splats, start a graph $\mathcal{G}$ by adding the projections as vertices.
Compute initial vertex candidates and their priority, add candidates to the queue.
while candidate vertex v_c exists in the queue **do**
  if $\mathcal{G}$ has vertex v s.t. $\|v - v_c\|_2 < d$ or v_c fails the projection check **then**
    Discard v_c.
  else if priority of v is not correct **then**
    Correct priority by pushing v_c back to the queue.
  else
    Add v_c and edges to its parent vertices to $\mathcal{G}$, update region borders. Compute new vertex candidates around v_c and their priorities, add them to the queue.
for each region $R \in \mathcal{R}$ **do**
  while length of region border ∂R is ≥ 3 and $< \partial_{\max}$ **do**
    Cut triangle t at the smallest border angle, add t to $\mathcal{T}$.

The experiments run on said repository are subdivided into three sections. In Section 1, we investigate the window size w by running the algorithm on the *Bottle Shampoo* with varying values for w. This motivates our standard parameter choice $w = 8$ as presented in the paper. Then, in Section 2, we discuss and illustrate how the triangulation of borders is done in detail. In Section 4, we present results for each model. Section 5 is dedicated to the investigation whether the output is sensitive to the choice of starting vertices. This includes:

- an image of the meshed model, as obtained by our algorithm,
- histograms showing the angle distribution, edge lengths distribution, and distribution of the triangle quality Q_t for the model,
- and the number of triangles and aggregated quality measures in tables.

See Section 5 of the paper for an explanation of these quantities. Note that the images and histograms displayed in Section 4 come from the output of our algorithm without applying a remeshing step. As in the paper, the best values achieved for the root mean square deviation E_{RMS}, for the quality Q_t its average Q_{avg}, and the root mean square deviation Q_{RMS} per model are highlighted. The table also shows values for a remeshed version of our results for comparison. Values are highlighted here if they improve those shown above.

Note that our algorithm produces a triangulation of edge lengths close to uniformity. This is reflected in the second histogram presented for each model, i.e., in the edge lengths distribution. The target edge length for all models is 0.2, which—by construction—is also the lowest edge length possible in the output of our algorithm. Larger edges are possible, but there is a significant spike at the target edge length 0.2. This insurance of a minimal edge length is the main reason why our algorithm does not perform best, but very close to best among the compared algorithms, when comparing average edge lengths in Tables 1 to 4 of the main paper. Because of the strict minimum at 0.2, there are no shorter edges that can bring the average closer to 0.2 again, cf. the discussion in Section 5 of the paper.

As the edges are all of very uniform length, the triangles are almost equilateral. This is noticeable by the large spike at 60° in the first histogram of each model, showing the angle distribution.

Note that a significant number of triangles t of the resulting triangulations actually achieve very high up to highest

quality possible, i.e., $0.99 < Q_t = 1$, and are thus sorted into the last bin of the respective histogram. The distribution of this quality is very tight across all models. See Section 5 of the paper for the definition of this quality measure.

In Section 5, we include additional data sets for a reasonable selection of models to illustrate the robustness of the algorithm. Therefore, we chose the *Wrench*, the *Lock*, and the *Bottle Shampoo* because of the features in contrast to the comparibly smooth *Toy Bear* shown in the paper and run the algorithm with eight different pairs of starting vertices. Further, we included the data sets corresponding to the *Toy Bear* for completeness. The data sets consist of significant characteristics including the total number of generated triangles $|\mathcal{T}|$, the maximum edge length $E_{\max}$, the average edge length E_{avg}, the root mean square deviation E_{RMS}, the minimum triangle quality $Q_{\min}$, the maximum triangle quality $Q_{\max}$, the average triangle quality Q_{avg}, and the root mean square deviation Q_{RMS}.

Finally, Sections 6 and 7 display a variety of point clouds as well as CAD models used to illustrate our advances in feature detection and preservation. The point clouds belong to the repository named above, while the CAD models are based on models priviously available at AIM@SHAPE. Their reconstructions are made by U. Reitebuch and they can be downloaded at [2]. This supplementary material contains all information not included in the paper for completeness. Next to histograms showing the distributions of angles, edge lengths, and triangle quality, we illustrate our findings with two different resolutions for the target edge length d. For point clouds, a table lists information like target edge length, feature angle (if chosen), number of vertices, number of triangles, as well as d_{avg}, $d_{\max}$, and d_{RMS} as defined in the original paper. In case of feature detection, we additionally list the number of detected feature segments and feature vertices. The CAD models come with a table listing the target edge length, the feature angle chosen by the user, the resulting number of vertices $|\mathcal{V}|$ and of triangles $|\mathcal{T}|$, the minimal angle $\alpha_{\min}$ achieved, the maximal angle $\alpha_{\max}$, the average angle α_{avg}, and the corresponding RMS value α_{RMS}. Further, the table contains the maximal edge length $E_{\max}$, the average edge length E_{avg} as well as the corresponsing RMS value E_{RMS}. In addition, we evaluate the quality measure introduced in the original article and collect the resulting values for $Q_{\min}$, $Q_{\max}$, Q_{avg}, and Q_{RMS}. As mentioned in the main article, we compare results achieved by running our algorithm to those achieved by running a certain routine implemented in Meshlab. For two models, the *Oloid* model and the *Body of Constant Width* model, we increased the number of iterations until there were no overfoldings occuring anymore. These overfoldings are not visible in the tables shown in Sections 7.2 and 7.4.

References

[1] Zhangjin Huang, Yuxin Wen, Zihao Wang, Jinjuan Ren, and Kui Jia. Surface reconstruction from point clouds: A survey and a benchmark. *arXiv preprint arXiv:2205.02413*, 2022.

[2] Ulrich Reitebuch. CAD Models. https://ms-math-computer.science/projects/guaranteed-smallest-edge-length-manifold-meshing.html, 2025.

Figure 1: Real-world scanned models as point clouds as presented in [1]. From left to right: *Bottle Shampoo*, *Bowl Chinese*, *Cloth Duck*, *Coffee Bottle Metal*, *Coffee Bottle Plastic*, *Cup*, *Flower Pot*, *Flower Pot 2*, *Gift Box*, *Lock*, *Mouse*, *Mug*, *Rabbit*, *Remote*, *Screw*, *Tape*, *Toy Bear*, *Toy Duck*, *Wrench*, *Xiao Jie Jie*.

1 Window Size

As mentioned in the paper, the algorithm asks for a window size w, which is used to limit tracing along borders in order to place the next vertex candidate. Experiments run with different window sizes show that the triangulation quality and the number of triangles obtain plateau from $w = 8$ onward. This makes $w = 8$ a reasonable choice for a reliable output with respect to the occurring lengths of borders before triangulating the created regions. See the result of the experiments in Figures 2 and 3. All experiments were run on the *Bottle Shampoo*.

On this model, the effect of changing the window sizes within this comparably small regime ([0,32]) is not measurable when considering the run time. That is on the one hand side because all these look-ups are constant-time as opposed to considering the entire border, which can grow towards an expected time of $\mathcal{O}(\sqrt{n})$ for n vertices placed. On the other hand size, traversing a border for a small number of vertices already suffices to find that the traversed points are on the same border region. Thus, an increased window size does not have any effect on these specific queries.

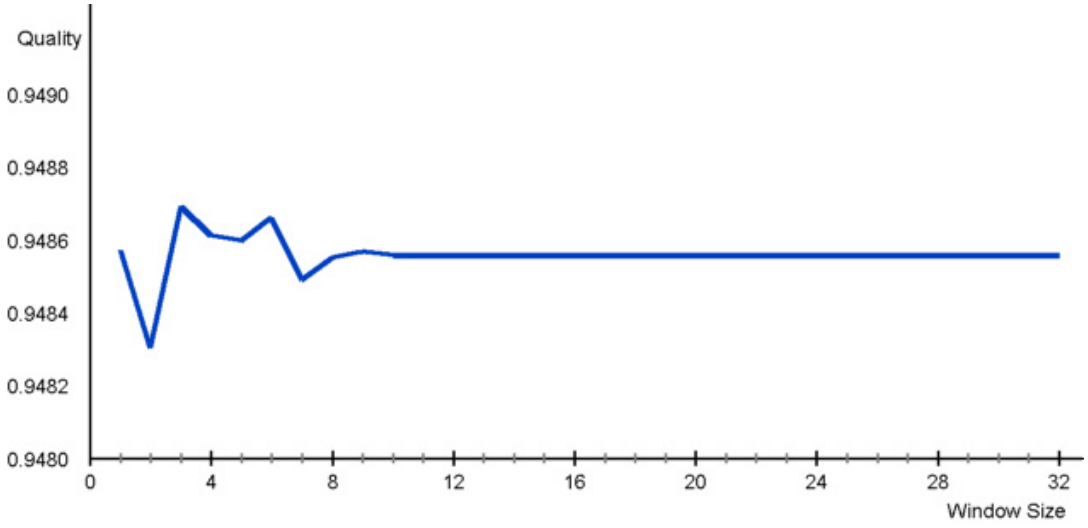

Figure 2: Quality Q_t for varying window sizes.

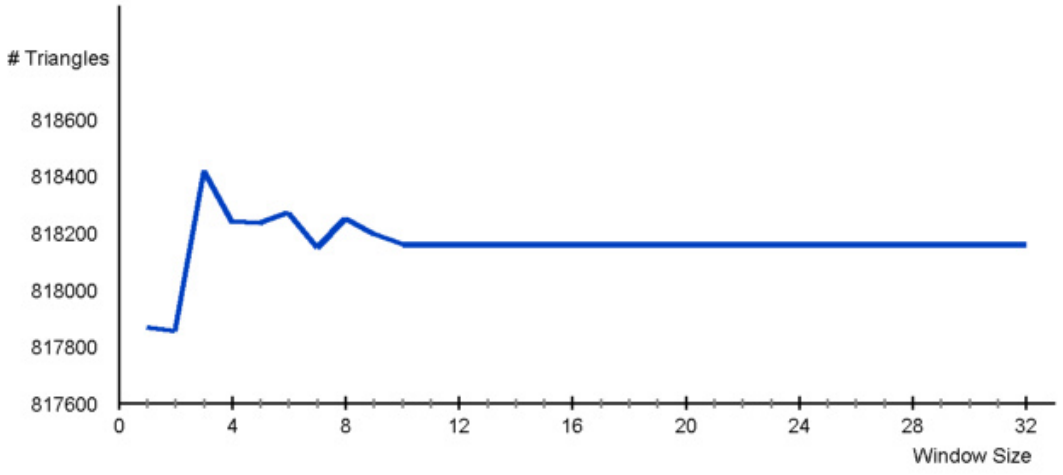

Figure 3: Number of triangles for varying window sizes.

The window size w influences the border length of the arising regions. As illustrated in Figure 7 in the article, a very small window size, i.e., $w = 0$, results in borders up to length 93 while increasing the window size to $w = 8$ reduces the border length to 11.

In contrast to the target edge length d chosen to illustrate the effect on the *Bottle Shampoo* in the paper, here, the target edge length is equal to 0.2 to conincide with the other experiments presented in the supplementary material. As shown in Figure 4, a bigger window size w prevents longer borders. Here, for $w = 0$, the longest border is of length 80 while for $w = 8$, there is no region of border length bigger than 20. Most resulting regions have a border length settled between 3 and 12 for both choices for w. Note that the histogram in Figure 4 has a log-scale y-axis. The obtained triangle quality stems to the largest extend from the placement of the vertices, rather than from triangulating regions with borders larger than 3. Even though changing the window size does not influence the run time significantly, it influences the visual aspects of the output, but the mesh quality after trigangulating the regions remains untouched as aforementioned.

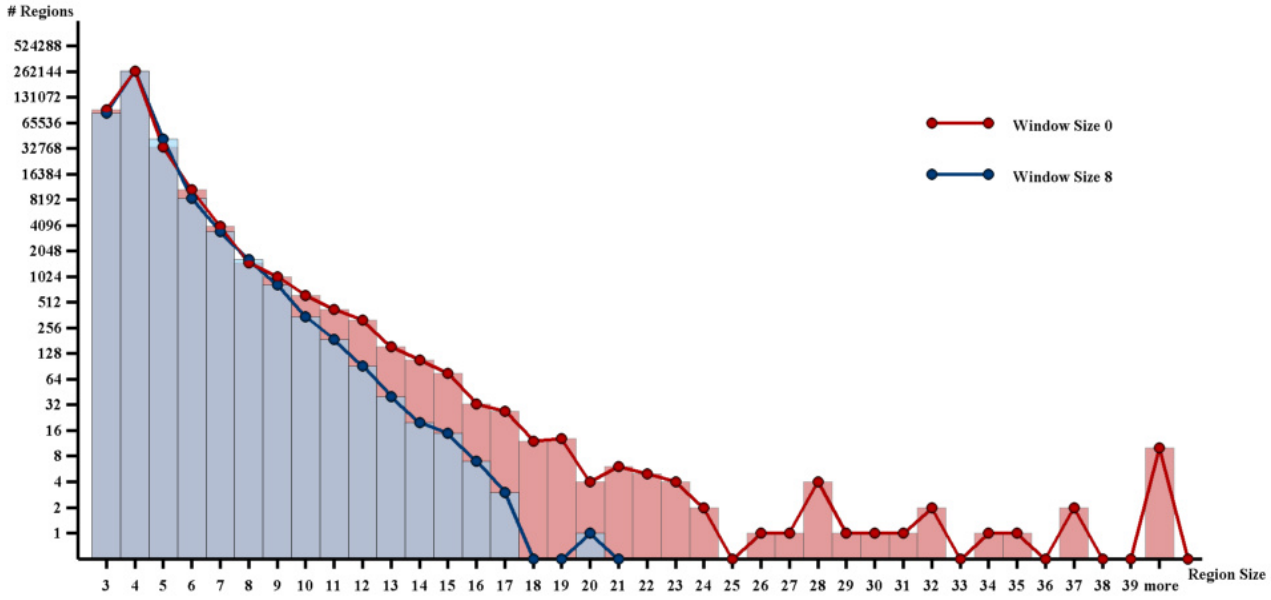

Figure 4: Region sizes for window sizes $w = 0$ (shown in blue) and $w = 8$ (shown in red) apllied to the *Bottle Shampoo*.

2 Triangulation of Borders

After the algorithm was run on a geometry, the final graph may contain region borders longer than 3. In order to obtain a triangular mesh, these have to be triangulated. During application of our algorithm, we assign to every vertex the normal n_b of the box the considered point is associated to as its vertex normal. Additionally, this box normal gives us a best fitting local approximation of the resconstructed surface. Hence, for each point p on a boundary ∂R, we project the pair of edges adjacent to p belonging to ∂R to the tangent plane T_p defined by the corresponding box normal n_b. From the set of oriented angles $\{\alpha_p \mid p \in \partial R\}$ made by the projected pairs of edges adjacent to p, we choose the smallest one and connect the two points p_ℓ and p_r adjacent to p by an edge. We repeat this process now with the new border $(\partial R \setminus \{(p_\ell, p), (p, p_r)\}) \cup \{(p_\ell, p_r)\}$ until the remaining border is of length 3.

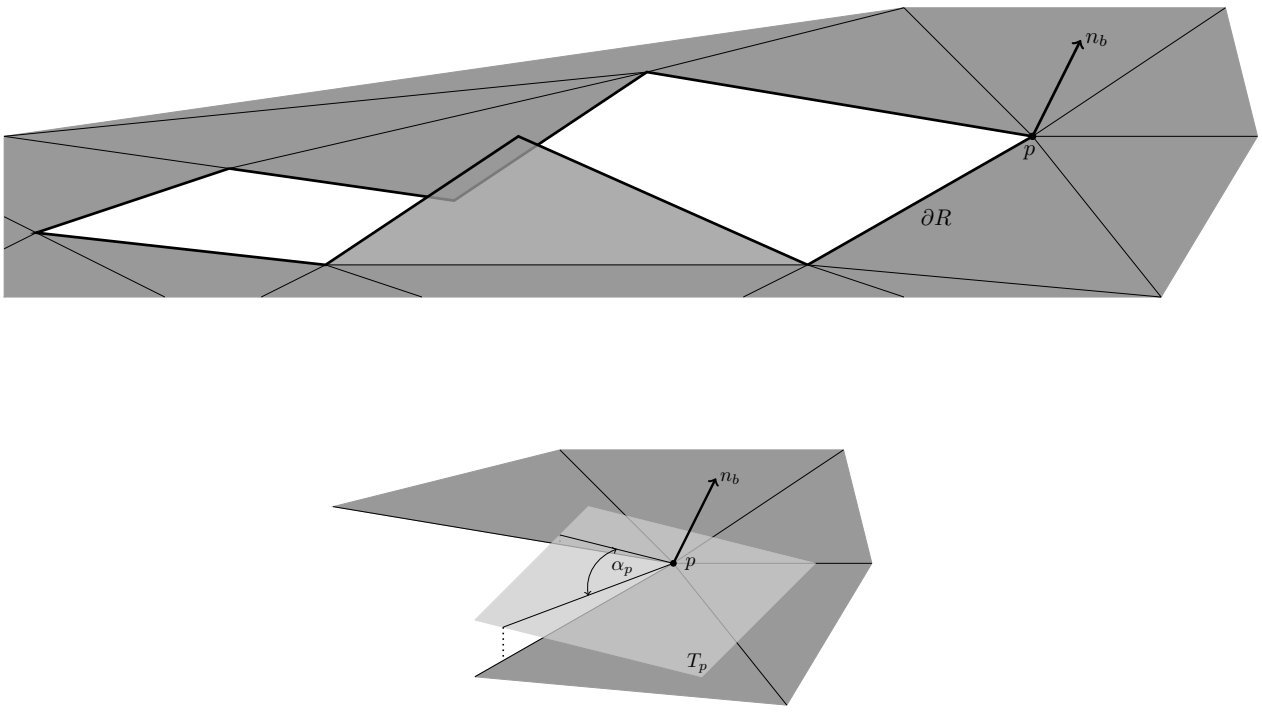

Figure 5: Top: Border ∂R to be triangulated. Bottom: Projection of border edges to tangent plane.

3 Handling of Noisy Data

In this section, we collect several observations made during the consideration of noisy data. For given reasons, the geometry sampled by a point cloud $\mathcal{P}$ with normal field $\mathcal{N}$ is a plane P. Without loss of generality, we assume this plane to be the x-y-plane. In the following, we analyze three different settings. In the first one, we solely assume the points in $\mathcal{P}$ to be noisy. Next, we assume the points of $\mathcal{P}$ to lie in P and the normals to be noisy. In the third case, we combine the two situations considered before.

Even though P is not a proper example fulfilling the properties listed in Section 3.1 in the paper, it allows us to demonstrate several thoughts because of its simple structure and well known properties. Since the reach ρ of P is undefined, the target edge length d may be chosen depending on the level of noise and the initial splat size s may be equal to d.

Noisy Points, Correct Normal Field

Here, we assume the points in $\mathcal{P}$ to come with some noise while the normal field is assumed to be correct. Hence, based on the assumptions made above, all normals are equal to $(0,0,1)^T \in \mathbb{R}^3$ and hence $\langle n_i, n_j \rangle = 1 > 0$. Set $\nu = \max_{i\in\{1,\dots,n\}} |(p_i)_z|$, where $(.)_z$ denotes the z-coordinate of $p_i \in \mathcal{P}$. Then, the two planes parallel to P at distance ν enclose $\mathcal{P}$. By construction, all generated splats lie between these two planes as well as all generated vertices. Especially, if $d > 2\nu$, no edges cross already existing ones under projection to the tangent plane, which is here the plane P itself, as described in Section 3.6 in the paper. Hence, after triangulating the occuring regions, the result is a graph above P and hence topologically correct.

Correct Points, Noisy Normals

Now, we assume the points in $\mathcal{P}$ to lie in P while the normals deviate by some angle $\alpha_i \in \left[0, \frac{\pi}{2}\right[$ from the correct normal $(0,0,1)^T$. Let $\alpha_{\max} = \max_{i\in\{1,\dots,n\}} \alpha_i$ denote the biggest deviation angle. Since the elements of $\mathcal{P}$ lie in P, but the normals deviate from the correct ones, the splats do not lie in P but stick out. Hence, in z-direction, the height of such a splat is bounded by $\nu_\alpha = s \sin(\alpha_{\max})$ and similar to the scenario described before, the splats are enclosed by two parallel planes determined by $\alpha_{\max}$. Additionally, the box normals do not deviate more from the correct normal than the noisy ones. For $d = 2\nu$, problems may occur while projecting the edges to the respective tangent plane. In order to prevent these faulty projections, choose $d > d_{\min} = 2\nu_\alpha \cos(\alpha_{\max})$.

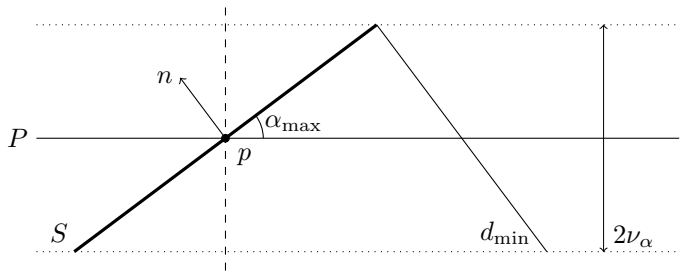

Noisy Points, Noisy Normals

Now, assuming both the points and the normals to be noisy, can be visualized as adding some offset in form of a translation into z-direction. This offset is given as $dz = \max_{i\in\{1,\dots,n\}} |(p_i)_z|$. Therefore, the distance of the bounding planes to P is given by $dz = \nu + \nu_\alpha$ and choose $d > 2dz \cos(\alpha_{\max})$.

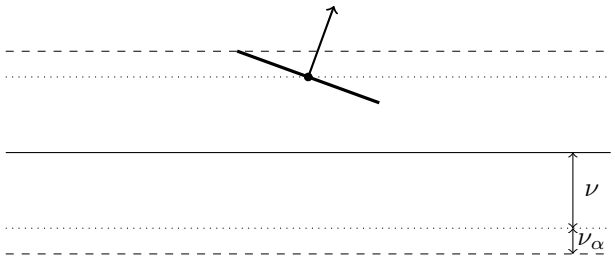

4 Collection of Models

4.1 *Bottle Shampoo*

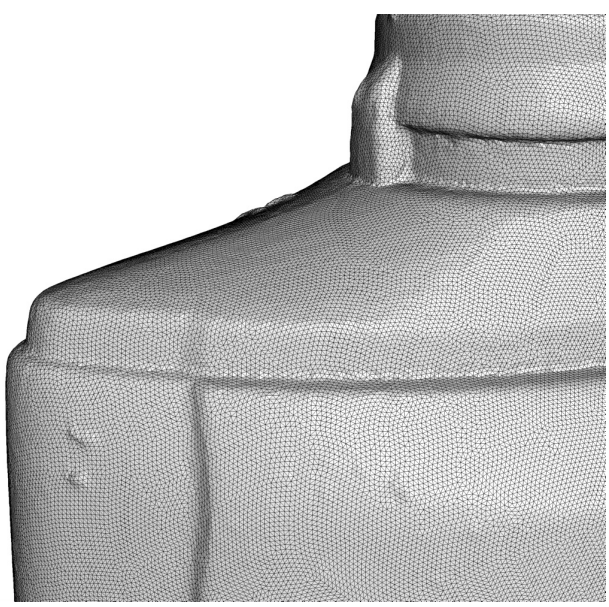

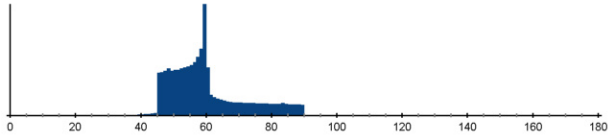

(a) Angle distribution, target=60°.

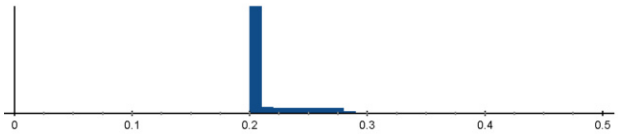

(b) Edge lengths distribution, target=0.2.

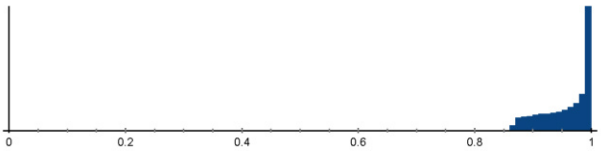

(c) Distribution of quality Q_t, target=1.0.

Figure 6: *Bottle Shampoo*.

Algorithm	$\lvert\mathcal{T}\rvert$	E_{avg}	E_{RMS}	Q_{avg}	Q_{RMS}
Adv. Front	1.209,546	0.1799	39.6	0.8247	16.0
Adv. Front (Re)	928,850	0.2028	15.3	0.9416	6.1
Poisson	16,280	1.2946	74.8	0.8760	12.3
Poisson (Re)	498,140	0.2657	38.6	0.9251	7.5
Poisson MG	150,770	0.5318	35.7	0.7204	33.7
Poisson MG (Re)	952,830	**0.2015**	16.3	0.9330	7.0
RIMLS	1,907,781	0.1499	35.8	0.7055	35.1
RIMLS (Re)	1,054,438	0.1905	19.3	0.9117	11.5
Scale Space	1,209,093	0.1798	39.1	0.8248	16.0
Scale Space (Re)	926,828	0.2028	15.2	0.9417	6.0
Voronoi	1,209,792	0.1799	52.3	0.8241	16.1
Voronoi (Re)	923,476	0.2044	20.8	0.9407	6.8
Ours	840,453	0.2131	**11.2**	**0.9577**	**4.5**
Ours (Re)	854,257	0.2098	**10.4**	**0.9701**	**3.8**

Table 1: Experimental results for the *Bottle Shampoo* from [1] (604,903 points).

4.2 *Bowl Chinese*

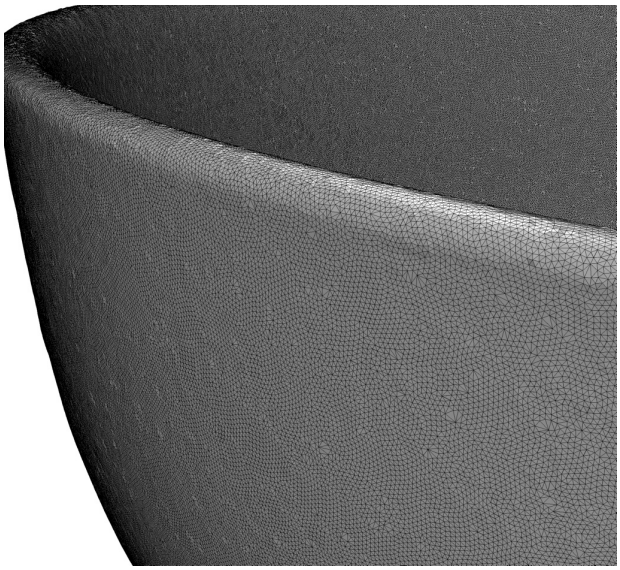

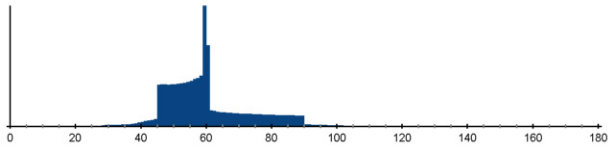

(a) Angle distribution, target=60°.

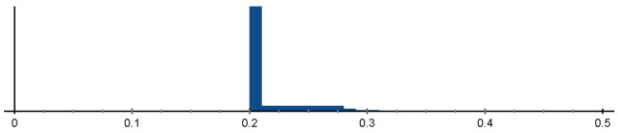

(b) Edge lengths distribution, target=0.2.

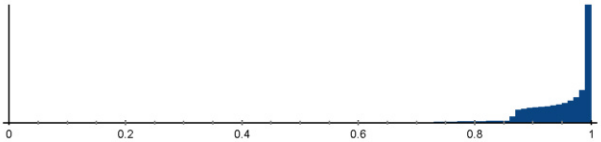

(c) Distribution of quality Q_t, target=1.0.

Figure 7: *Bowl Chinese*.

Algorithm	$\lvert\mathcal{T}\rvert$	E_{avg}	E_{RMS}	Q_{avg}	Q_{RMS}
Adv. Front	1,212,636	0.2920	38.2	0.8045	18.6
Adv. Front (Re)	2,407,002	0.2038	15.4	0.9405	6.2
Poisson	13,584	2.3850	63.2	0.8845	11.7
Poisson (Re)	637,488	0.3732	40.8	0.9301	6.9
Poisson MG	503,458	0.4710	39.8	0.7062	37.1
Poisson MG (Re)	2,409,076	0.2050	17.7	0.9223	7.9
RIMLS	6,458,589	0.1331	40.4	0.6877	39.6
RIMLS (Re)	2,441,143	0.2023	15.4	0.9394	6.3
Scale Space	1,093,339	0.2779	34.9	0.8054	18.7
Scale Space (Re)	1,947,592	**0.2006**	16.1	0.9351	7.3
Voronoi	1,212,636	0.2916	38.4	0.8042	18.7
Voronoi (Re)	2,398,584	0.2039	15.3	0.9405	**6.1**
Ours	2,137,650	0.2167	**14.8**	**0.9485**	6.2
Ours (Re)	2,246,434	0.2093	**11.4**	**0.9665**	**4.3**

Table 2: Experimental results for the *Bowl Chinese* from [1] (606,320 points).

4.3 *Cloth Duck*

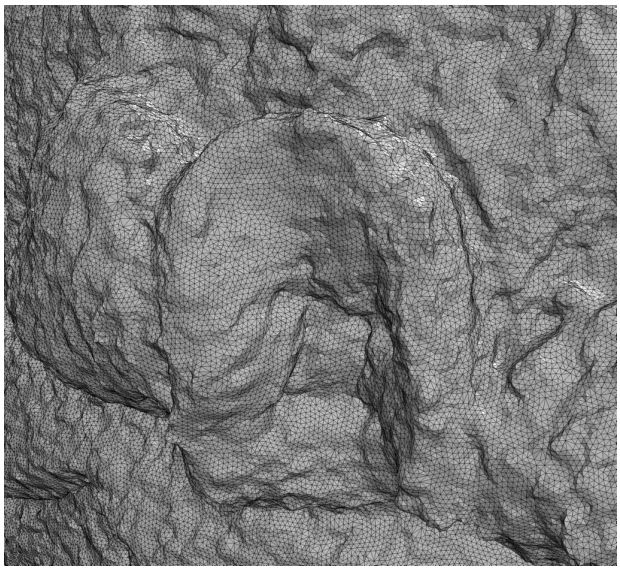

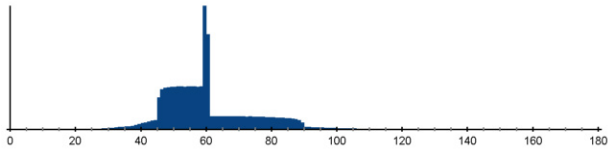

(a) Angle distribution, target=60°.

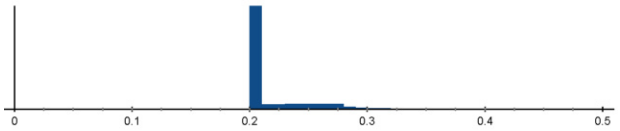

(b) Edge lengths distribution, target=0.2.

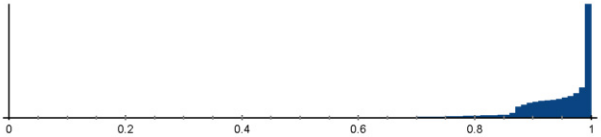

(c) Distribution of quality Q_t, target=1.0.

Figure 8: *Cloth Duck*.

Algorithm	$\lvert\mathcal{T}\rvert$	E_{avg}	E_{RMS}	Q_{avg}	Q_{RMS}
Adv. Front	2,037,574	0.1839	40.1	0.8143	17.3
Adv. Front (Re)	1,739,214	0.1965	19.4	0.9179	9.5
Poisson	147,940	0.6300	44.3	0.8805	12.0
Poisson (Re)	1,488,112	0.2068	17.5	0.9311	7.2
Poisson MG	419,614	0.4086	38.5	0.7160	36.0
Poisson MG (Re)	1,463,018	0.2093	18.7	0.9154	8.8
RIMLS	5,878,521	0.1154	39.9	0.6919	38.9
RIMLS (Re)	1,728,371	**0.1978**	20.1	0.9143	12.7
Scale Space	2,036,816	0.1839	40.0	0.8139	17.4
Scale Space (Re)	1,735,814	0.1965	19.3	0.9179	9.5
Voronoi	2,037,270	0.1767	41.8	0.8067	18.1
Voronoi (Re)	1,514,160	0.2027	**15.4**	0.9407	**6.3**
Ours	1,435,604	0.2181	15.7	**0.9454**	6.6
Ours (Re)	1,535,058	0.2089	**12.5**	**0.9592**	**4.8**

Table 3: Experimental results for the *Cloth Duck* from [1] (1,018,891 points).

4.4 *Coffee Bottle Metal*

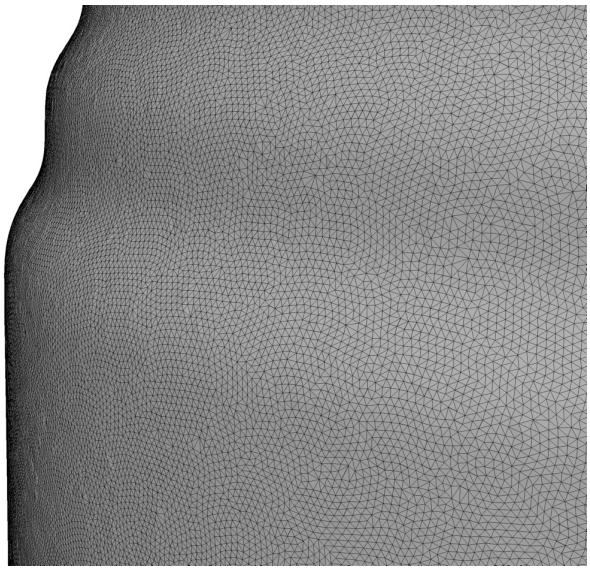

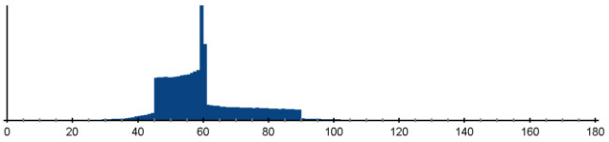

(a) Angle distribution, target=60°.

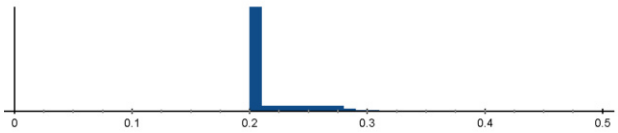

(b) Edge lengths distribution, target=0.2.

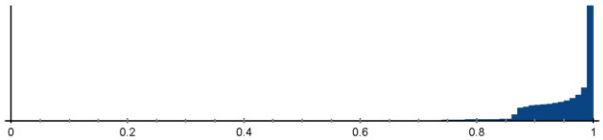

(c) Distribution of quality Q_t, target=1.0.

Figure 9: *Coffee Bottle Metal.*

Algorithm	$\lvert\mathcal{T}\rvert$	E_{avg}	E_{RMS}	Q_{avg}	Q_{RMS}
Adv. Front	1,211,290	0.2204	44.2	0.8036	18.4
Adv. Front (Re)	1,423,429	0.2029	15.2	0.9416	6.1
Poisson	25,842	1.2170	84.0	0.8743	12.4
Poisson (Re)	670,954	0.2805	41.6	0.9254	7.5
Poisson MG	249,103	0.5440	46.4	0.7265	33.0
Poisson MG (Re)	1,657,210	0.2097	20.8	0.9143	8.0
RIMLS	3,024,537	0.1477	35.4	0.7107	34.4
RIMLS (Re)	1,489,387	**0.1986**	18.0	0.9229	10.1
Scale Space	1,197,246	0.2188	43.4	0.8039	18.5
Scale Space (Re)	1,379,802	0.2021	15.5	0.9397	6.5
Voronoi	1,211,618	0.2198	52.6	0.8021	18.6
Voronoi (Re)	1,412,630	0.2043	21.1	0.9411	6.6
Ours	1,260,935	0.2162	**14.0**	**0.9494**	**5.9**
Ours (Re)	1,317,181	0.2095	**11.4**	**0.9661**	**4.3**

Table 4: Experimental results for the *Coffee Bottle Metal* from [1] (605,826 points).

4.5 *Coffee Bottle Plastic*

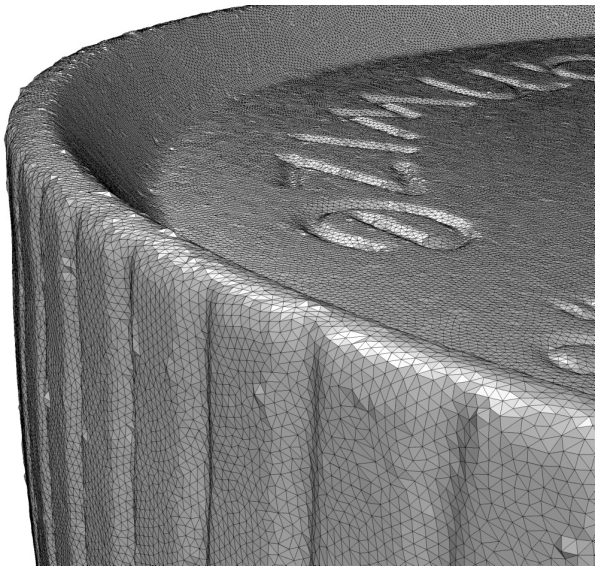

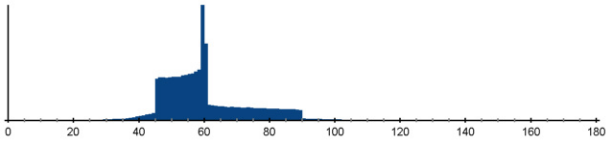

(a) Angle distribution, target=60°.

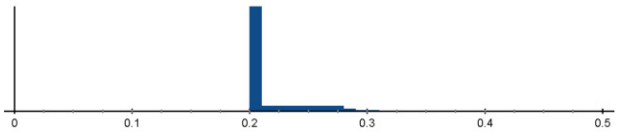

(b) Edge lengths distribution, target=0.2.

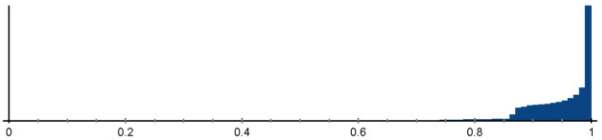

(c) Distribution of quality Q_t, target=1.0.

Figure 10: *Coffee Bottle Plastic.*

Algorithm	$\lvert\mathcal{T}\rvert$	E_{avg}	E_{RMS}	Q_{avg}	Q_{RMS}
Adv. Front	1,218,482	0.2128	45.7	0.8049	18.2
Adv. Front (Re)	1,359,038	0.2027	15.2	0.9417	6.1
Poisson	29,206	1.1586	76.5	0.8636	13.2
Poisson (Re)	746,200	0.2557	44.2	0.9205	7.8
Poisson MG	576,442	0.3273	35.4	0.7267	33.2
Poisson MG (Re)	1,530,906	0.1931	16.1	0.9134	**5.8**
RIMLS	7,438,789	0.0922	35.9	0.7121	34.8
RIMLS (Re)	1,308,171	0.2070	15.5	0.9373	6.5
Scale Space	1,204,794	0.2112	45.0	0.8050	18.2
Scale Space (Re)	1,316,070	**0.2019**	15.5	0.9398	6.4
Voronoi	1,218,482	0.2114	46.4	0.8028	18.4
Voronoi (Re)	1,341,154	0.2032	15.1	0.9422	6.0
Ours	1,203,156	0.2162	**14.0**	**0.9495**	**5.8**
Ours (Re)	1,257,141	0.2094	**11.4**	**0.9659**	**4.3**

Table 5: Experimental results for the *Coffee Bottle Plastic* from [1] (609,243 points).

4.6 *Cup*

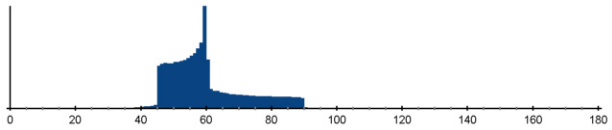

(a) Angle distribution, target=60°.

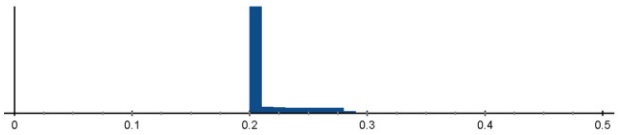

(b) Edge lengths distribution, target=0.2.

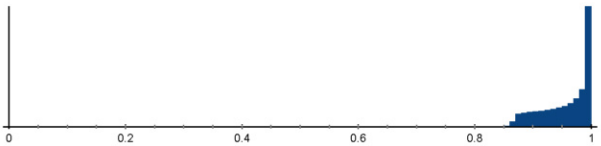

(c) Distribution of quality Q_t, target=1.0.

Figure 11: *Cup*.

Algorithm	$\lvert\mathcal{T}\rvert$	E_{avg}	E_{RMS}	Q_{avg}	Q_{RMS}
Adv. Front	2,820,618	0.1038	21.5	0.8978	6.1
Adv. Front (Re)	711,716	0.2032	15.0	0.9430	5.9
Poisson	31,450	0.8540	63.3	0.8744	12.5
Poisson (Re)	660,134	0.2110	19.5	0.9297	7.2
Poisson MG	605,996	0.2330	39.6	0.7050	37.2
Poisson MG (Re)	692,170	0.2064	17.1	0.9323	7.0
RIMLS	7,815,640	0.0658	40.2	0.6880	39.4
RIMLS (Re)	713,396	0.2040	16.5	0.9295	7.1
Scale Space	2,820,618	0.1038	21.5	0.8978	6.1
Scale Space (Re)	712,010	**0.2031**	15.0	0.9430	5.9
Voronoi	2,820,618	0.1035	21.6	0.8976	6.2
Voronoi (Re)	664,994	0.2097	14.8	0.9420	6.1
Ours	645,670	0.2133	**11.3**	**0.9570**	**4.5**
Ours (Re)	657,232	0.2099	**10.6**	**0.9694**	**3.9**

Table 6: Experimental results for the *Cup* from [1] (1,410,309 points).

4.7 *Flower Pot*

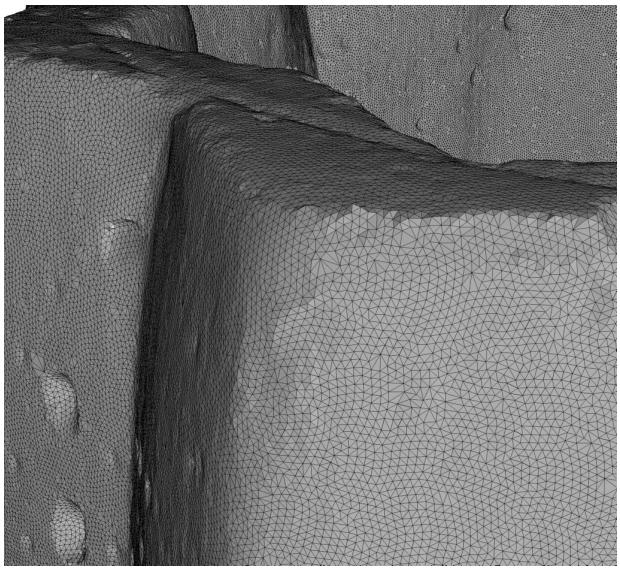

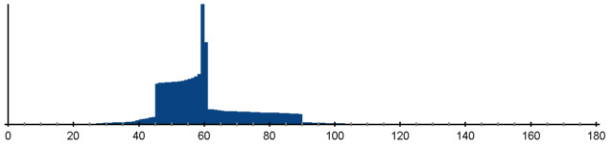

(a) Angle distribution, target=60°.

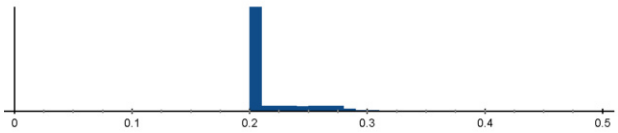

(b) Edge lengths distribution, target=0.2.

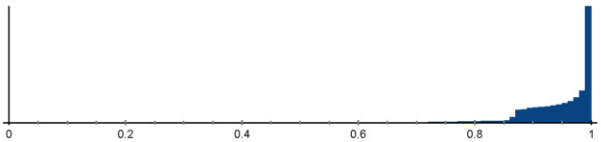

(c) Distribution of quality Q_t, target=1.0.

Figure 12: *Flower Pot.*

Algorithm	$\lvert\mathcal{T}\rvert$	E_{avg}	E_{RMS}	Q_{avg}	Q_{RMS}
Adv. Front	1,226,042	0.2780	46.1	0.8010	19.0
Adv. Front (Re)	2,304,698	0.2043	15.7	0.9376	6.5
Poisson	30,656	1.5601	67.1	0.8589	13.6
Poisson (Re)	1,164,952	0.2722	41.4	0.9157	8.1
Poisson MG	747,300	0.3767	36.6	0.7235	33.9
Poisson MG (Re)	2,296,376	0.2052	16.7	0.9247	8.2
RIMLS	9,625,452	0.1063	37.2	0.7050	36.1
RIMLS (Re)	2,252,713	0.2064	**15.1**	0.9410	**6.2**
Scale Space	1,057,169	0.2555	42.0	0.8017	19.1
Scale Space (Re)	1,644,152	**0.1997**	16.8	0.9288	8.3
Voronoi	1,226,042	0.2764	46.6	0.7996	19.2
Voronoi (Re)	2,284,266	0.2045	15.7	0.9378	6.4
Ours	2,052,950	0.2170	**15.1**	**0.9476**	6.4
Ours (Re)	2,161,017	0.2095	**11.7**	**0.9642**	**4.6**

Table 7: Experimental results for the *Flower Pot* from [1] (613,021 points).

4.8 *Flower Pot 2*

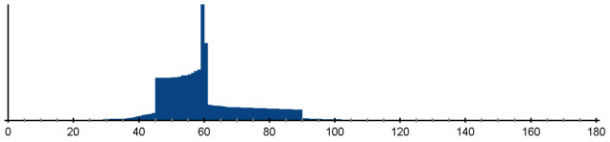

(a) Angle distribution, target=60°.

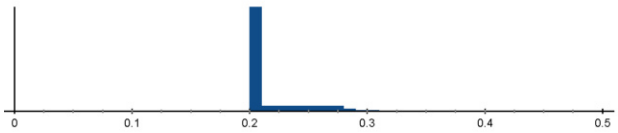

(b) Edge lengths distribution, target=0.2.

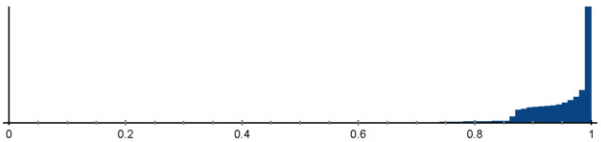

(c) Distribution of quality Q_t, target=1.0.

Figure 13: *Flower Pot 2*.

Algorithm	$\lvert\mathcal{T}\rvert$	E_{avg}	E_{RMS}	Q_{avg}	Q_{RMS}
Adv. Front	2,826,864	0.2135	38.1	0.8136	17.3
Adv. Front (Re)	3,001,322	0.2031	15.1	0.9425	**5.9**
Poisson	26,436	1.7814	80.3	0.8668	13.0
Poisson (Re)	1,062,612	0.3053	56.0	0.9198	7.7
Poisson MG	640,912	0.4605	36.4	0.7400	32.7
Poisson MG (Re)	3,016,388	0.2043	18.7	0.9180	8.4
RIMLS	8,225,140	0.1302	37.0	0.7205	35.3
RIMLS (Re)	2,939,770	0.2053	15.4	0.9392	6.7
Scale Space	2,815,621	0.2130	37.8	0.8138	17.2
Scale Space (Re)	2,969,237	**0.2028**	15.2	0.9418	6.1
Voronoi	2,826,862	0.2133	38.2	0.8133	17.3
Voronoi (Re)	2,985,334	0.2034	15.0	0.9428	**5.9**
Ours	2,661,776	0.2162	**14.0**	**0.9494**	**5.9**
Ours (Re)	2,782,563	0.2094	**11.4**	**0.9662**	**4.3**

Table 8: Experimental results for the *Flower Pot 2* from [1] (1,413,342 points).

4.9 *Gift Box*

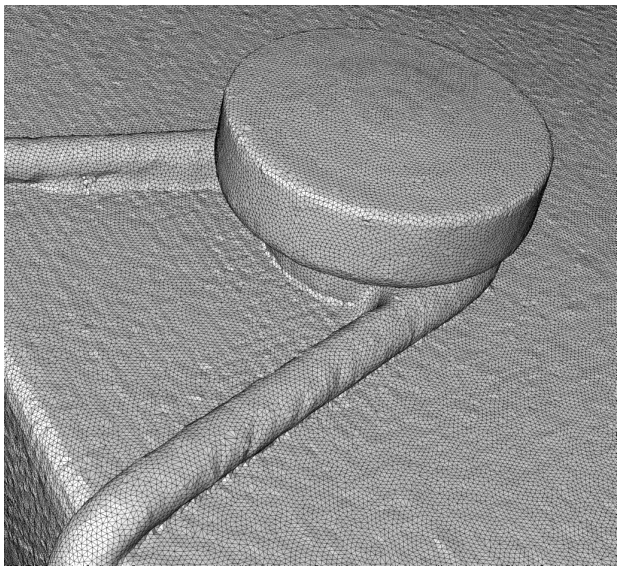

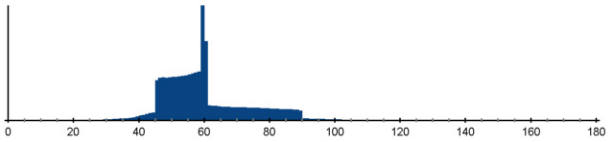

(a) Angle distribution, target=60°.

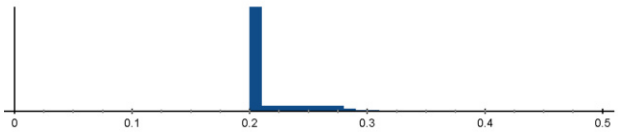

(b) Edge lengths distribution, target=0.2.

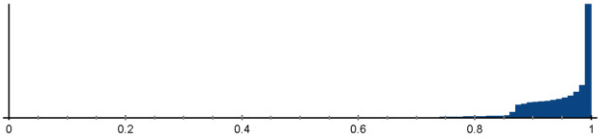

(c) Distribution of quality Q_t, target=1.0.

Figure 14: *Gift Box*.

Algorithm	$\lvert\mathcal{T}\rvert$	E_{avg}	E_{RMS}	Q_{avg}	Q_{RMS}
Adv. Front	3,063,655	0.1809	40.0	0.8313	15.7
Adv. Front (Re)	2,400,932	0.2022	15.5	0.9409	6.3
Poisson	68,578	0.7763	130.2	0.8681	12.9
Poisson (Re)	845,348	0.2990	62.8	0.9242	7.7
Poisson MG	400,500	0.6026	61.4	0.7877	24.7
Poisson MG (Re)	3,389,028	0.2185	31.1	0.9126	8.5
RIMLS	4,649,233	0.1531	74.9	0.7641	28.0
RIMLS (Re)	4,648,407	0.1522	75.2	0.7761	25.7
Scale Space	3,059,551	0.1808	39.9	0.8313	15.7
Scale Space (Re)	2,395,066	**0.2020**	15.6	0.9405	6.4
Voronoi	3,063,361	0.1796	40.7	0.8297	15.9
Voronoi (Re)	2,360,337	0.2028	15.3	0.9415	6.3
Ours	2,115,895	0.2164	**14.2**	**0.9487**	**6.1**
Ours (Re)	2,211,935	0.2096	**11.8**	**0.9639**	**4.5**

Table 9: Experimental results for the *Gift Box* from [1] (1,532,008 points).

4.10 *Lock*

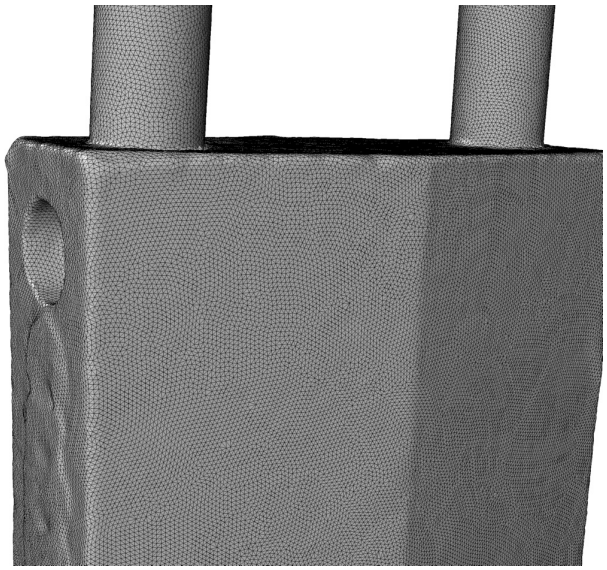

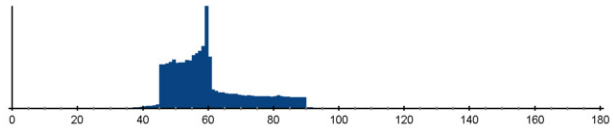

(a) Angle distribution, target=60°.

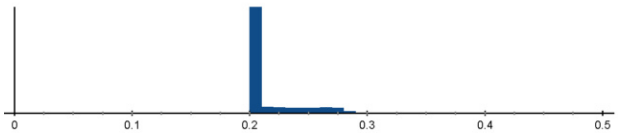

(b) Edge lengths distribution, target=0.2.

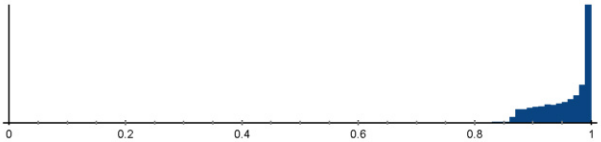

(c) Distribution of quality Q_t, target=1.0.

Figure 15: *Lock*.

Algorithm	$\lvert\mathcal{T}\rvert$	E_{avg}	E_{RMS}	Q_{avg}	Q_{RMS}
Adv. Front	668,388	0.1152	18.3	0.9227	6.6
Adv. Front (Re)	211,646	**0.2035**	15.0	0.9434	5.9
Poisson	12,598	0.6966	79.2	0.8654	13.1
Poisson (Re)	153,344	0.2318	33.9	0.9241	7.7
Poisson MG	201,226	0.2201	36.3	0.7118	34.4
Poisson MG (Re)	204,718	0.2078	17.0	0.9319	6.9
RIMLS	2,585,492	0.0620	36.7	0.6966	36.1
RIMLS (Re)	212,924	0.2043	16.9	0.9251	7.4
Scale Space	668,388	0.1152	18.3	0.9227	6.6
Scale Space (Re)	211,572	0.2036	15.0	0.9434	5.8
Voronoi	668,388	0.1147	18.5	0.9224	6.7
Voronoi (Re)	201,296	0.2089	15.5	0.9313	7.4
Ours	192,260	0.2136	**11.6**	**0.9560**	**4.6**
Ours (Re)	196,018	0.2101	**11.0**	**0.9673**	**4.3**

Table 10: Experimental results for the *Lock* from [1] (334,194 points).

4.11 *Mouse*

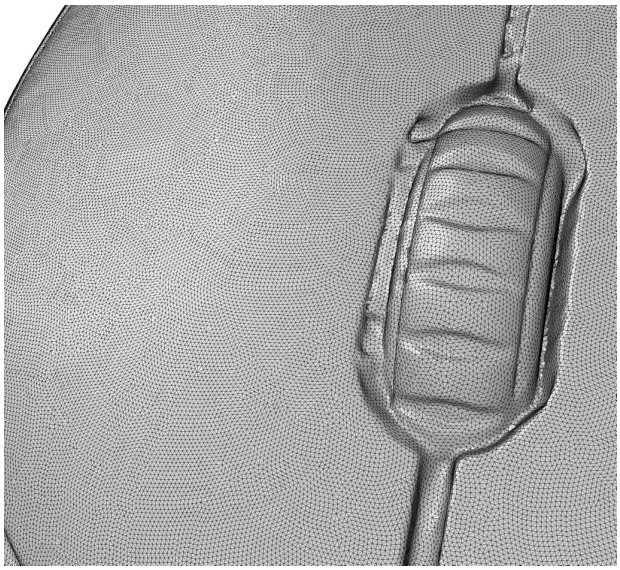

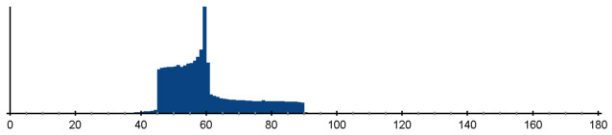

(a) Angle distribution, target=60°.

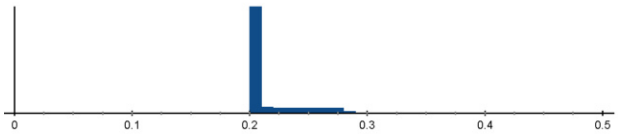

(b) Edge lengths distribution, target=0.2.

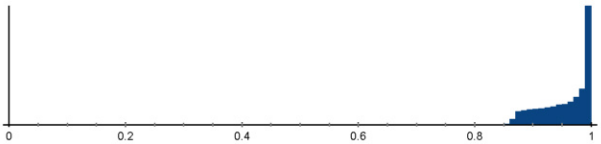

(c) Distribution of quality Q_t, target=1.0.

Figure 16: *Mouse*.

Algorithm	$\lvert\mathcal{T}\rvert$	E_{avg}	E_{RMS}	Q_{avg}	Q_{RMS}
Adv. Front	2,564,191	0.1265	26.6	0.8806	8.2
Adv. Front (Re)	947,782	0.2036	15.2	0.9421	6.2
Poisson	33,934	0.8160	97.7	0.8711	12.9
Poisson (Re)	585,622	0.2521	34.8	0.9298	7.3
Poisson MG	265,630	0.4047	38.4	0.7125	35.7
Poisson MG (Re)	894,136	0.2108	18.2	0.9190	8.5
RIMLS	3,409,562	0.1145	39.1	0.6910	37.9
RIMLS (Re)	979,361	**0.1984**	22.2	0.9083	17.9
Scale Space	2,563,854	0.1265	26.6	0.8805	8.2
Scale Space (Re)	948,202	0.2035	15.2	0.9420	6.3
Voronoi	2,564,340	0.1262	26.9	0.8801	8.3
Voronoi (Re)	881,846	0.2103	14.2	0.9464	6.2
Ours	862,392	0.2134	**11.5**	**0.9562**	**4.7**
Ours (Re)	878,134	0.2100	**10.9**	**0.9676**	**4.3**

Table 11: Experimental results for the *Mouse* from [1] (1,282,234 points).

4.12 *Mug*

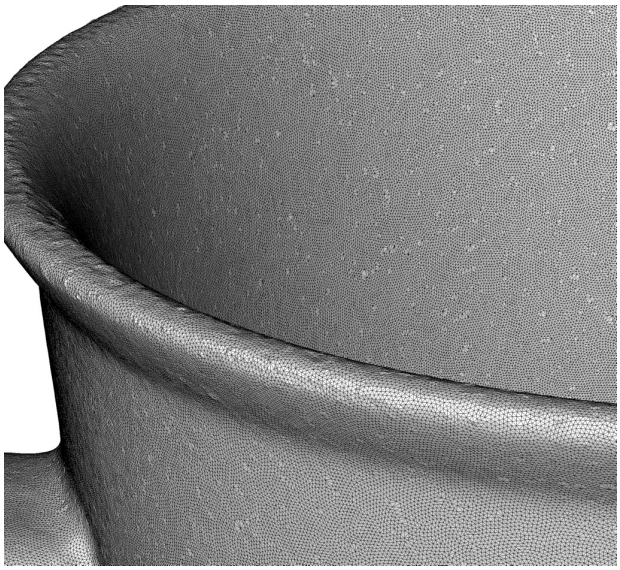

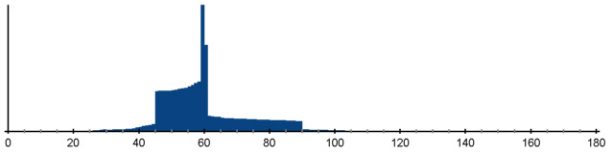

(a) Angle distribution, target=60°.

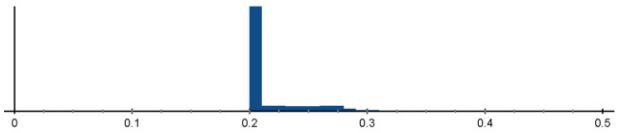

(b) Edge lengths distribution, target=0.2.

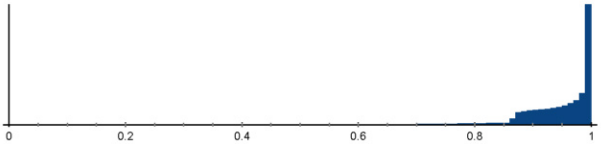

(c) Distribution of quality Q_t, target=1.0.

Figure 17: *Mug*.

Algorithm	$\lvert\mathcal{T}\rvert$	E_{avg}	E_{RMS}	Q_{avg}	Q_{RMS}
Adv. Front	1,212,626	0.3419	43.8	0.7999	19.1
Adv. Front (Re)	3,387,245	0.2049	**15.9**	0.9362	6.5
Poisson	16,520	2.5528	65.7	0.8822	11.8
Poisson (Re)	811,746	0.3845	47.9	0.9259	7.3
Poisson MG	550,330	0.5340	35.8	0.7233	33.3
Poisson MG (Re)	3,500,438	0.2016	16.1	0.9340	6.8
RIMLS	7,059,114	0.1507	36.3	0.7062	35.3
RIMLS (Re)	3,901,787	0.1919	16.8	0.9230	**6.1**
Scale Space	840,041	0.2861	36.8	0.8014	19.4
Scale Space (Re)	1,606,753	**0.1985**	17.3	0.9240	8.9
Voronoi	1,212,628	0.3413	44.0	0.7995	19.2
Voronoi (Re)	3,376,934	0.2050	**15.9**	0.9362	6.5
Ours	3,011,551	0.2175	16.2	**0.9470**	6.7
Ours (Re)	3,190,711	0.2093	**11.7**	**0.9646**	**4.6**

Table 12: Experimental results for the *Mug* from [1] (606,322 points).

4.13 *Rabbit*

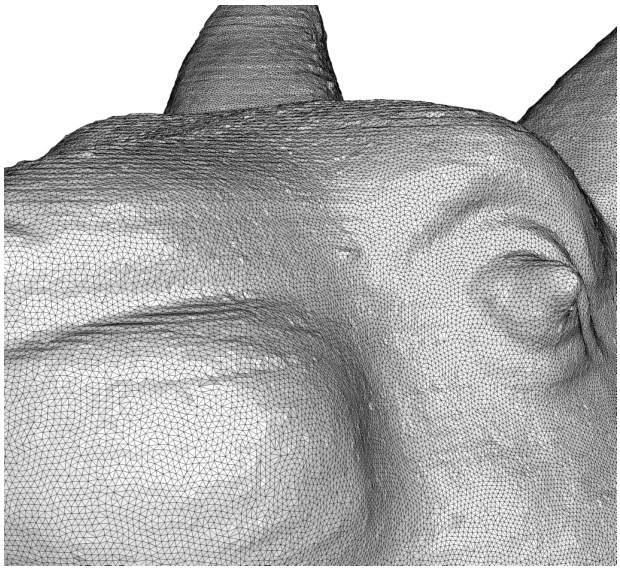

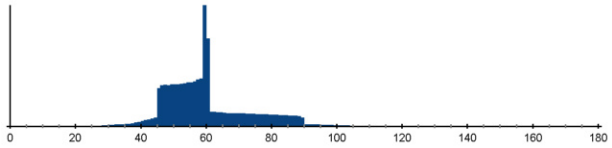

(a) Angle distribution, target=60°.

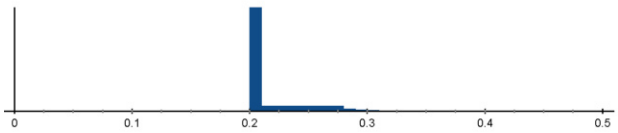

(b) Edge lengths distribution, target=0.2.

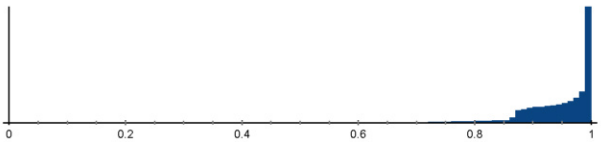

(c) Distribution of quality Q_t, target=1.0.

Figure 18: *Rabbit*.

Algorithm	$\lvert\mathcal{T}\rvert$	E_{avg}	E_{RMS}	Q_{avg}	Q_{RMS}
Adv. Front	4,046,178	0.1563	45.4	0.7782	19.9
Adv. Front (Re)	2,370,715	0.2006	16.5	0.9337	7.2
Poisson	79,654	0.9804	60.4	0.8767	12.5
Poisson (Re)	1,851,254	0.2215	29.1	0.9264	7.5
Poisson MG	293,676	0.5974	38.4	0.7154	35.8
Poisson MG (Re)	2,559,026	0.1931	16.6	0.9216	**6.1**
RIMLS	3,573,629	0.1692	38.8	0.6973	38.1
RIMLS (Re)	2,631,908	0.1868	27.0	0.8500	22.9
Scale Space	4,041,938	0.1561	45.1	0.7782	19.9
Scale Space (Re)	2,357,012	**0.2005**	16.6	0.9332	7.3
Voronoi	4,046,157	0.1552	45.6	0.7767	20.0
Voronoi (Re)	2,323,985	0.2014	15.9	0.9374	6.5
Ours	2,039,974	0.2173	**15.1**	**0.9470**	6.4
Ours (Re)	2,152,626	0.2093	**11.8**	**0.9636**	**4.5**

Table 13: Experimental results for the *Rabbit* from [1] (2,023,131 points).

4.14 *Remote*

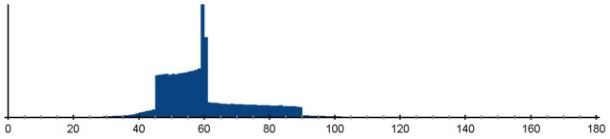

(a) Angle distribution, target=60°.

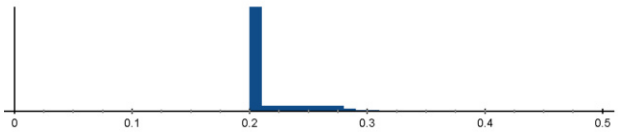

(b) Edge lengths distribution, target=0.2.

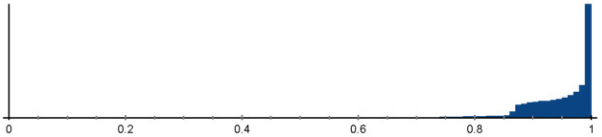

(c) Distribution of quality Q_t, target=1.0.

Figure 19: *Romote*.

Algorithm	$\lvert\mathcal{T}\rvert$	E_{avg}	E_{RMS}	Q_{avg}	Q_{RMS}
Adv. Front	1,211,452	0.1681	40.7	0.8298	15.9
Adv. Front (Re)	826,007	0.2023	15.5	0.9405	6.3
Poisson	37,808	0.7858	78.8	0.8603	13.5
Poisson (Re)	603,656	0.2306	31.2	0.9232	7.7
Poisson MG	132,682	0.5261	37.1	0.7352	34.0
Poisson MG (Re)	829,026	**0.2014**	16.5	0.9318	7.3
RIMLS	1,691,586	0.1490	37.4	0.7162	36.6
RIMLS (Re)	1,006,124	0.1834	22.0	0.8900	15.7
Scale Space	1,211,373	0.1681	40.7	0.8298	15.9
Scale Space (Re)	825,804	0.2023	15.5	0.9404	6.3
Voronoi	1,211,428	0.1667	41.5	0.8275	16.1
Voronoi (Re)	806,808	0.2034	15.3	0.9415	6.2
Ours	726,550	0.2164	**14.0**	**0.9488**	**5.9**
Ours (Re)	760,465	0.2094	**11.5**	**0.9654**	**4.4**

Table 14: Experimental results for the *Remote* from [1] (608,874 points).

4.15 *Screw*

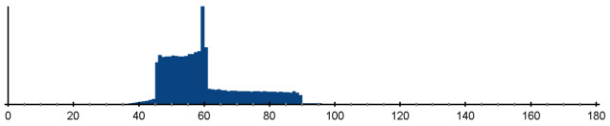

(a) Angle distribution, target=60°.

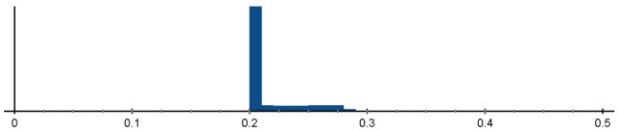

(b) Edge lengths distribution, target=0.2.

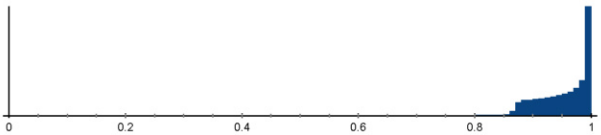

(c) Distribution of quality Q_t, target=1.0.

Figure 20: *Screw*.

Algorithm	$\lvert\mathcal{T}\rvert$	E_{avg}	E_{RMS}	Q_{avg}	Q_{RMS}
Adv. Front	990,307	0.1102	23.3	0.8999	8.9
Adv. Front (Re)	283,248	0.2028	15.7	0.9397	6.5
Poisson	72,344	0.3693	56.8	0.8624	12.9
Poisson (Re)	268,408	0.2069	18.9	0.9271	7.5
Poisson MG	126,076	0.3162	39.7	0.7102	37.1
Poisson MG (Re)	297,510	0.1962	17.0	0.9176	8.6
RIMLS	1,687,736	0.0895	40.7	0.6873	40.0
RIMLS (Re)	284,956	**0.2023**	19.1	0.9228	12.4
Scale Space	990,296	0.1102	23.3	0.8999	8.9
Scale Space (Re)	283,400	0.2027	15.7	0.9397	6.6
Voronoi	990,314	0.1065	23.9	0.8970	9.3
Voronoi (Re)	252,708	0.2079	15.4	0.9394	6.6
Ours	254,936	0.2144	**12.1**	**0.9531**	**5.0**
Ours (Re)	261,268	0.2103	**11.6**	**0.9633**	**4.4**

Table 15: Experimental results for the *Screw* from [1] (495,182 points).

4.16 *Tape*

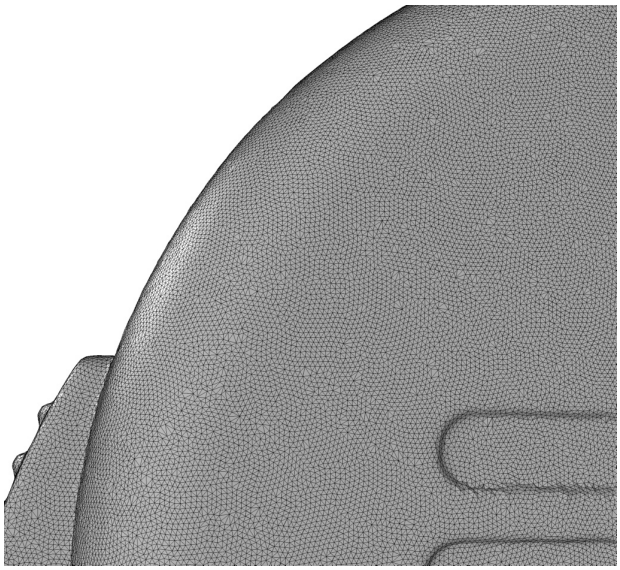

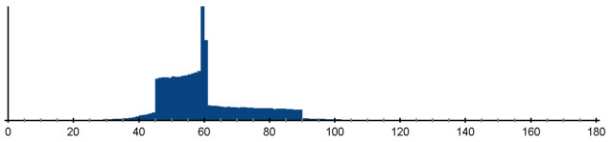

(a) Angle distribution, target=60°.

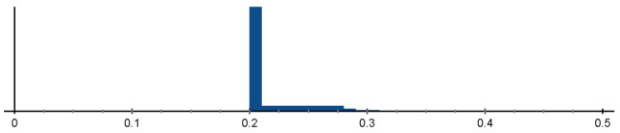

(b) Edge lengths distribution, target=0.2.

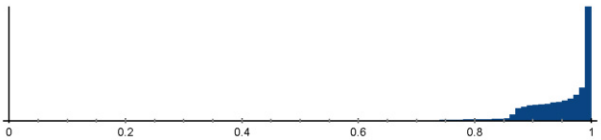

(c) Distribution of quality Q_t, target=1.0.

Figure 21: *Tape*.

Algorithm	$\lvert\mathcal{T}\rvert$	E_{avg}	E_{RMS}	Q_{avg}	Q_{RMS}
Adv. Front	1,022,926	0.1693	47.8	0.8250	16.4
Adv. Front (Re)	704,575	0.2028	16.2	0.9385	7.1
Poisson	27,660	0.8333	83.3	0.8650	13.2
Poisson (Re)	474,692	0.2364	38.2	0.9203	7.9
Poisson MG	280,190	0.3369	35.6	0.7373	32.3
Poisson MG (Re)	773,900	0.1962	16.2	0.9097	6.1
RIMLS	3,577,797	0.0950	35.9	0.2486	34.5
RIMLS (Re)	680,432	0.2055	16.2	0.9357	7.6
Scale Space	1,021,944	0.1685	41.5	0.8255	16.2
Scale Space (Re)	698,119	**0.2025**	15.5	0.9405	6.3
Voronoi	1,023,090	0.1680	46.9	0.8234	16.5
Voronoi (Re)	690,444	0.2042	16.5	0.9400	6.8
Ours	616,091	0.2162	**14.0**	**0.9491**	**5.8**
Ours (Re)	643,856	0.2097	**11.9**	**0.9633**	**4.7**

Table 16: Experimental results for the *Tape* from [1] (511,569 points).

4.17 *Toy Bear*

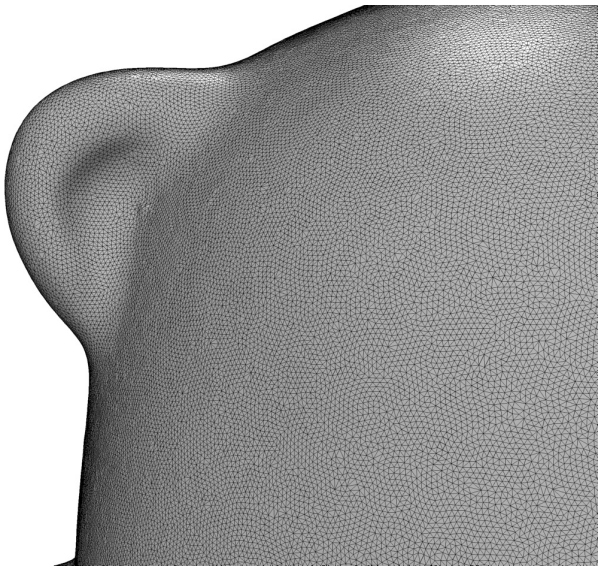

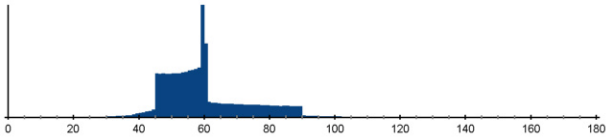

(a) Angle distribution, target=60°.

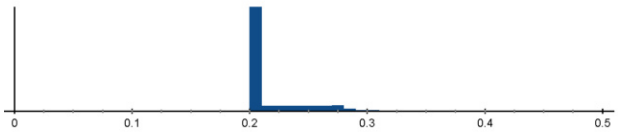

(b) Edge lengths distribution, target=0.2.

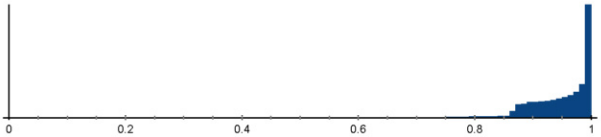

(c) Distribution of quality Q_t, target=1.0.

Figure 22: *Toy Bear*.

Algorithm	$\lvert\mathcal{T}\rvert$	E_{avg}	E_{RMS}	Q_{avg}	Q_{RMS}
Adv. Front	1,214,998	0.1474	36.3	0.8474	13.9
Adv. Front (Re)	629,138	0.2024	15.2	0.9418	6.0
Poisson	20,134	1.0381	54.7	0.8882	11.7
Poisson (Re)	530,374	0.2193	22.8	0.9293	7.3
Poisson MG	432,268	0.2585	39.5	0.2623	37.1
Poisson MG (Re)	629,508	**0.2021**	15.0	0.9436	6.1
RIMLS	5,548,226	0.0730	40.0	0.6910	39.3
RIMLS (Re)	618,531	0.2049	16.2	0.9322	6.8
Scale Space	1,214,990	0.1474	36.3	0.8474	13.9
Scale Space (Re)	628,848	0.2025	15.2	0.9417	6.0
Voronoi	1,214,996	0.1471	36.5	0.8471	13.9
Voronoi (Re)	616,160	0.2041	15.0	0.9427	5.9
Ours	555,490	0.2159	**13.5**	**0.9499**	**5.6**
Ours (Re)	578,730	0.2096	**11.5**	**0.9657**	**4.3**

Table 17: Experimental results for the *Toy Bear* from [1] (607,501 points).

4.18 *Toy Duck*

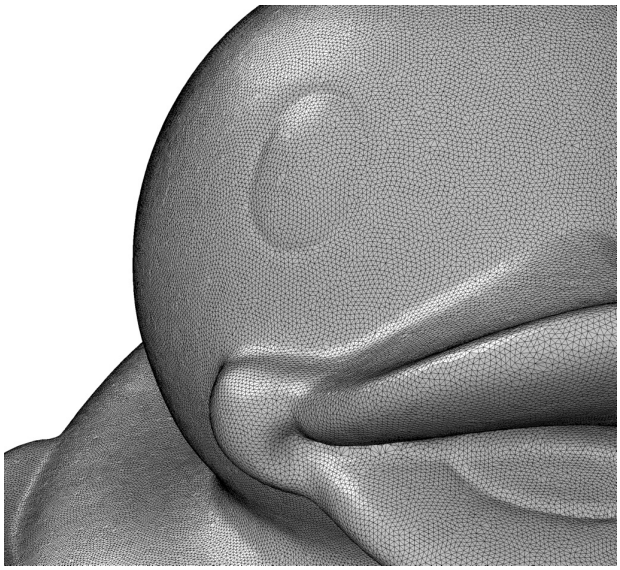

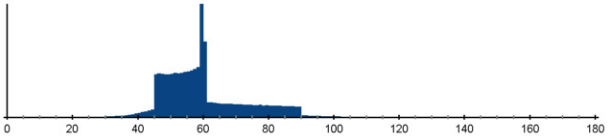

(a) Angle distribution, target=60°.

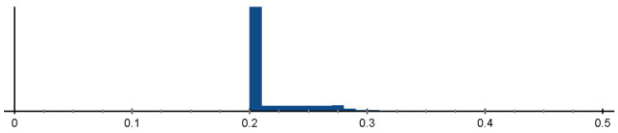

(b) Edge lengths distribution, target=0.2.

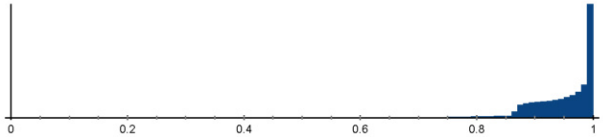

(c) Distribution of quality Q_t, target=1.0.

Figure 23: *Toy Duck*.

Algorithm	$\lvert\mathcal{T}\rvert$	E_{avg}	E_{RMS}	Q_{avg}	Q_{RMS}
Adv. Front	1,208,620	0.1523	36.7	0.8347	14.9
Adv. Front (Re)	664,788	0.**2023**	15.3	0.9412	6.1
Poisson	18,238	1.1320	51.1	0.8876	11.8
Poisson (Re)	578,760	0.2158	20.9	0.9337	7.0
Poisson MG	503,882	0.2456	39.4	0.7090	36.9
Poisson MG (Re)	642,274	0.2064	16.8	0.9315	6.8
RIMLS	6,470,657	0.0694	40.1	0.6910	39.4
RIMLS (Re)	655,847	0.2044	16.4	0.9310	7.0
Scale Space	1,208,618	0.1523	36.7	0.8347	14.9
Scale Space (Re)	664,854	**0.2023**	15.3	0.9412	6.1
Voronoi	1,208,620	0.1520	36.8	0.8345	14.9
Voronoi (Re)	654,288	0.2036	15.1	0.9422	6.0
Ours	585,744	0.2160	**13.6**	**0.9497**	**5.7**
Ours (Re)	610,908	0.2095	**11.5**	**0.9658**	**4.3**

Table 18: Experimental results for the *Toy Duck* from [1] (604,312 points).

4.19 *Wrench*

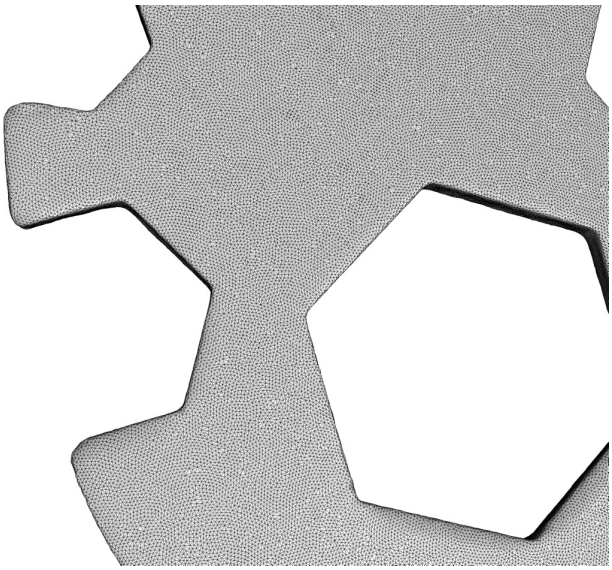

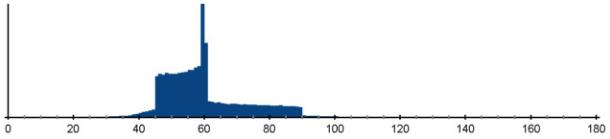

(a) Angle distribution, target=60°.

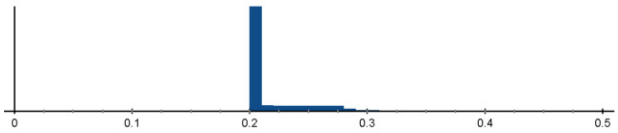

(b) Edge lengths distribution, target=0.2.

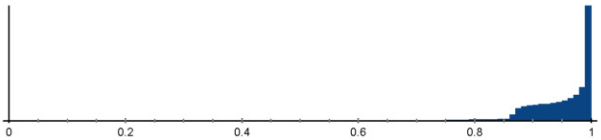

(c) Distribution of quality Q_t, target=1.0.

Figure 24: *Wrench*.

Algorithm	$\lvert\mathcal{T}\rvert$	E_{avg}	E_{RMS}	Q_{avg}	Q_{RMS}
Adv. Front	1,219,826	0.1335	33.7	0.8538	12.6
Adv. Front (Re)	516,056	**0.2020**	15.5	0.9401	6.2
Poisson	26,428	0.6729	99.7	0.8469	14.2
Poisson (Re)	300,868	0.2535	37.5	0.9190	7.9
Poisson MG	66,946	0.5781	31.9	0.7818	26.0
Poisson MG (Re)	496,824	0.2054	15.1	0.9358	6.8
RIMLS	801,420	0.1656	31.2	0.7667	28.2
RIMLS (Re)	638,096	0.1808	20.6	0.8739	13.4
Scale Space	1,219,826	0.1335	33.7	0.8538	12.6
Scale Space (Re)	516,184	**0.2020**	15.4	0.9403	6.2
Voronoi	1,219,826	0.1326	34.3	0.8543	12.7
Voronoi (Re)	503,056	0.2037	15.4	0.9402	6.2
Ours	454,492	0.2157	**13.3**	**0.9508**	**5.5**
Ours (Re)	472,946	0.2095	**11.5**	**0.9655**	**4.4**

Table 19: Experimental results for the *Wrench* from [1] (609,911 points).

4.20 *Xiao Jie Jie*

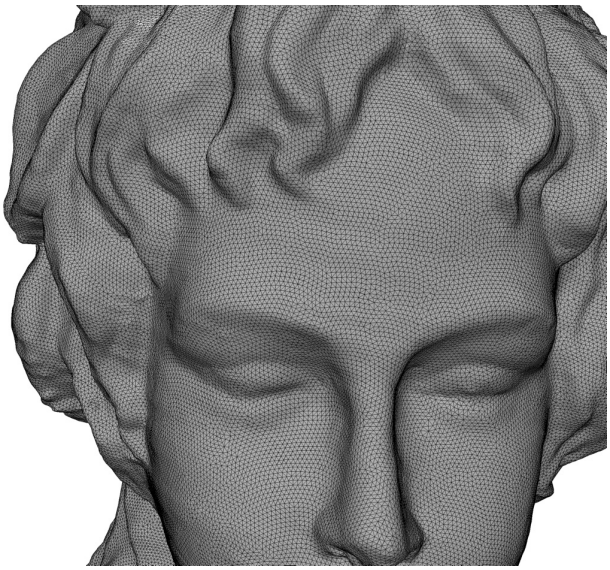

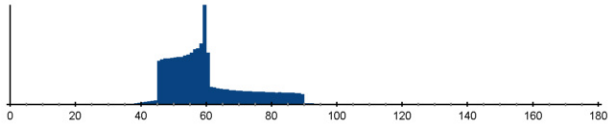

(a) Angle distribution, target=60°.

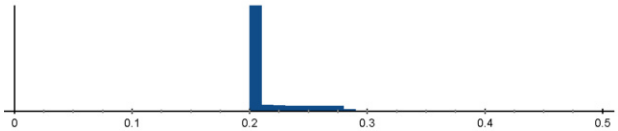

(b) Edge lengths distribution, target=0.2.

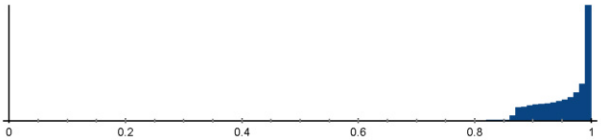

(c) Distribution of quality Q_t, target=1.0.

Figure 25: *Xiao Jie Jie*.

Algorithm	$\lvert\mathcal{T}\rvert$	E_{avg}	E_{RMS}	Q_{avg}	Q_{RMS}
Adv. Front	2,473,735	0.1198	27.2	0.8755	9.3
Adv. Front (Re)	811,986	**0.2037**	15.0	0.9433	6.0
Poisson	87,740	0.5677	55.9	0.8785	12.2
Poisson (Re)	755,538	0.2097	21.0	0.9321	7.1
Poisson MG	200,446	0.4316	39.7	0.7043	37.7
Poisson MG (Re)	786,370	0.2073	18.7	0.9152	8.7
RIMLS	2,528,244	0.1219	40.2	0.6833	40.0
RIMLS (Re)	1,066,017	0.1703	37.3	0.7956	34.3
Scale Space	2,473,712	0.1198	27.2	0.8750	9.3
Scale Space (Re)	812,416	**0.2037**	15.0	0.9432	6.0
Voronoi	2,473,692	0.1186	27.5	0.8751	9.4
Voronoi (Re)	753,938	0.2094	14.4	0.9463	5.8
Ours	739,325	0.2138	**11.6**	**0.9557**	**4.6**
Ours (Re)	754,086	0.2101	**11.2**	**0.9663**	**4.4**

Table 20: Experimental results for the *Xiao Jie Jie* from [1] (1,236,884 points).

5 Robustness of the Algorithm

For all models, we chose the same target edge length $d = 0.2$.

5.1 *Toy Bear*

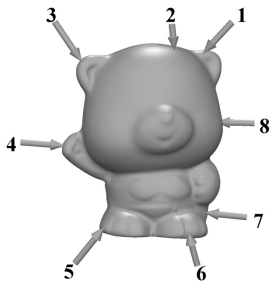

Pair	$\lvert\mathcal{T}\rvert$	$E_{\max}$	E_{avg}	E_{RMS}	$Q_{\min}$	$Q_{\max}$	Q_{avg}	Q_{RMS}
1	555,750	0.5395	0.2157	13.5	0.4817	1.0	0.9504	5.6
2	555,768	0.5151	0.2157	13.5	0.4465	1.0	0.9504	5.6
3	555,508	0.5107	0.2158	13.5	0.3856	1.0	0.9499	5.6
4	555,736	0.5229	0.2158	13.5	0.4164	1.0	0.9503	5.6
5	555,504	0.5489	0.2158	13.5	0.3950	1.0	0.9501	5.6
6	555,396	0.5466	0.2158	13.5	0.4358	1.0	0.9500	5.6
7	555,554	0.6009	0.2158	13.5	0.4632	1.0	0.9502	5.6
8	555,592	0.5493	0.2158	13.5	0.4253	1.0	0.9501	5.6

Figure 26: *Toy Bear* with eight different pairs of starting vertices and evaluation of results achieved.

5.2 *Wrench*

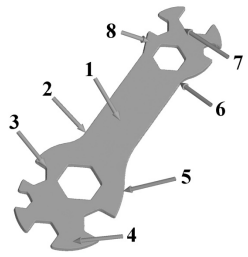

Pair	$\lvert\mathcal{T}\rvert$	$E_{\max}$	E_{avg}	E_{RMS}	$Q_{\min}$	$Q_{\max}$	Q_{avg}	Q_{RMS}
1	454,510	0.4911	0.2156	13.3	0.4748	1.0	0.9507	5.5
2	454,630	0.4905	0.2156	13.3	0.4528	1.0	0.9507	5.5
3	454,550	0.4724	0.2156	13.3	0.4645	1.0	0.9506	5.5
4	454,520	0.5160	0.2156	13.3	0.4499	1.0	0.9505	5.5
5	454,618	0.4747	0.2156	13.3	0.4817	1.0	0.9507	5.5
6	454,514	0.5056	0.2156	13.3	0.4862	1.0	0.9507	5.5
7	454,544	0.4684	0.2156	13.2	0.3887	1.0	0.9506	5.5
8	454,762	0.5033	0.2155	13.2	0.5011	1.0	0.9510	5.5

Figure 27: *Wrench* with eight different pairs of starting vertices and evaluation of results achieved.

5.3 *Lock*

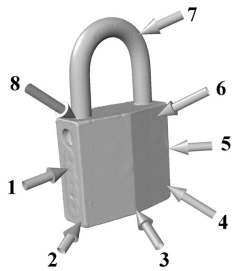

Pair	$\lvert\mathcal{T}\rvert$	$E_{\max}$	E_{avg}	E_{RMS}	$Q_{\min}$	$Q_{\max}$	Q_{avg}	Q_{RMS}
1	192,308	0.4502	0.2136	11.5	0.5373	1.0	0.9561	4.6
2	192,280	0.3997	0.2136	11.5	0.5811	1.0	0.9558	4.6
3	192,558	0.4296	0.2134	11.6	0.5936	1.0	0.9566	4.7
4	192,708	0.4168	0.2132	11.4	0.5858	1.0	0.9575	4.5
5	192,430	0.4172	0.2134	11.5	0.5642	1.0	0.9566	4.6
6	192,016	0.4162	0.2138	11.7	0.5568	1.0	0.9549	4.6
7	192,256	0.4237	0.2136	11.5	0.5630	1.0	0.9562	4.6
8	192,130	0.4380	0.2137	11.6	0.4729	1.0	0.9554	4.6

Figure 28: *Lock* with eight different pairs of starting vertices and evaluation of results achieved.

5.4 *Bottle Shampoo*

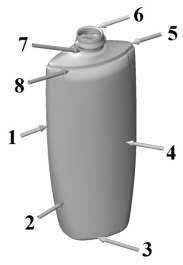

Pair	$\lvert\mathcal{T}\rvert$	$E_{\max}$	E_{avg}	E_{RMS}	$Q_{\min}$	$Q_{\max}$	Q_{avg}	Q_{RMS}
1	818,160	0.5702	0.2165	14.2	0.4270	1.0	0.9484	6.0
2	818,167	0.5499	0.2164	14.2	0.4349	1.0	0.9486	5.9
3	817,997	0.5734	0.2165	14.3	0.3969	1.0	0.9485	6.0
4	818,122	0.5664	0.2165	14.2	0.3876	1.0	0.9485	6.0
5	818,025	0.5918	0.2165	14.2	0.3937	1.0	0.9483	6.0
6	818,261	0.5841	0.2164	14.2	0.2944	1.0	0.9486	5.9
7	817,836	0.5619	0.2165	14.2	0.3317	1.0	0.9483	6.0
8	818,137	0.5893	0.2165	14.2	0.3811	1.0	0.9485	6.0

Figure 29: *Bottle Shampoo* with eight different pairs of starting vertices and evaluation of results achieved.

6 Collection of Point Clouds for Feature Detection

6.1 *Lock*

Figure 30: *Lock*. Left: Meshes point cloud without feature detection. Middle: Point cloud with features detected for $\vartheta = 60°$ and target edge length $d = 0.8$. Right: Meshed point cloud with features detected before.

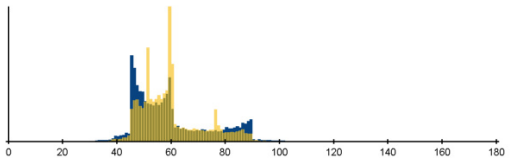

(a) Angle distribution, target=60°.

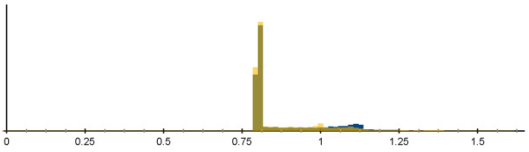

(b) Edge lengths distribution, target=0.8.

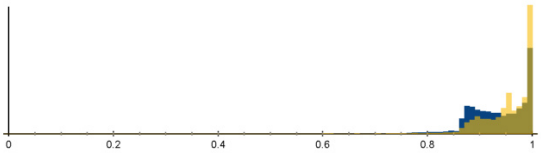

(c) Distribution of quality Q_t, target=1.0.

Figure 31: Histograms for remeshed *Lock*, with (blue) and without (yellow) feature detection, $\vartheta = 60°$.

d	ϑ	$\lvert\mathcal{V}\rvert$	$\lvert\mathcal{T}\rvert$	d_{avg}	$d_{\max}$	d_{RMS}	|feature segments|	|feature vertices|
0.8	—	5,951	11,902	0.016	0.4609	193.6	—	—
0.8	60°	5,837	11,674	0.011	0.2963	142.6	473,115	423

Table 21: Comparison of results achieved for *Lock*, with and without feature detection.

6.2 *Remote*

Figure 32: *Remote*. Left: Meshes point cloud without feature detection. Middle: Point cloud with features detected for $\vartheta = 50°$ and target edge length $d = 0.8$. Right: Meshed point cloud with features detected before.

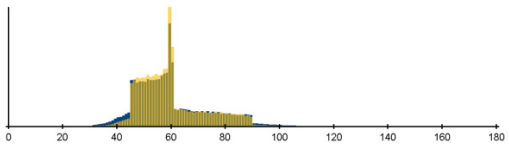

(a) Angle distribution, target=60°.

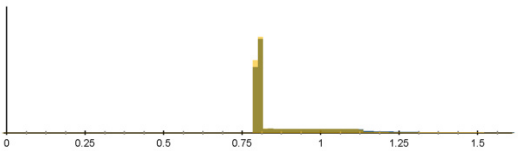

(b) Edge lengths distribution, target=0.8.

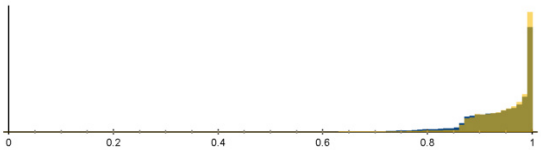

(c) Distribution of quality Q_t, target=1.0.

Figure 33: Histograms for remeshed *Remote*, with (blue) and without (yellow) feature detection, $\vartheta = 50°$.

d	ϑ	$\lvert\mathcal{V}\rvert$	$\lvert\mathcal{T}\rvert$	d_{avg}	$d_{\max}$	d_{RMS}	|feature segments|	|feature vertices|
0.8	—	22,595	45,186	0.0296	0.2963	192.5	—	—
0.8	50°	22,239	44,474	0.0178	0.4879	162.7	1,249,250	2,031

Table 22: Comparison of results achieved for *Remote*, with and without feature detection.

6.3 *Screw*

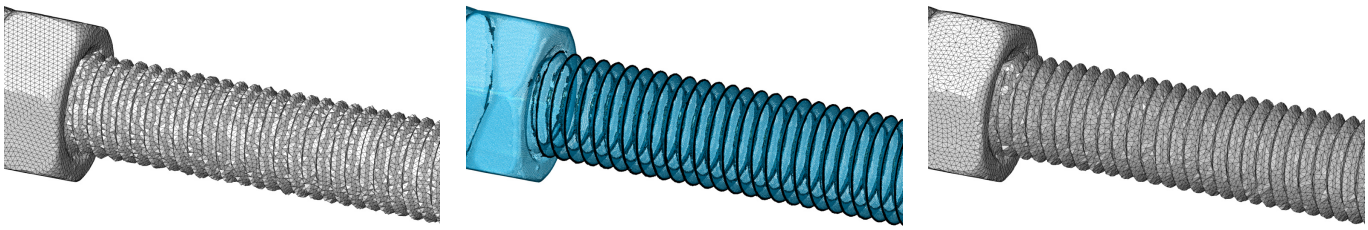

Figure 34: *Screw*. Left: Meshes point cloud without feature detection. Middle: Point cloud with features detected for $\vartheta = 90°$ and target edge length $d = 0.6$. Right: Meshed point cloud with features detected before.

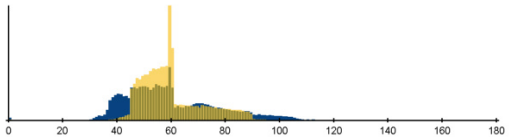

(a) Angle distribution, target=60°.

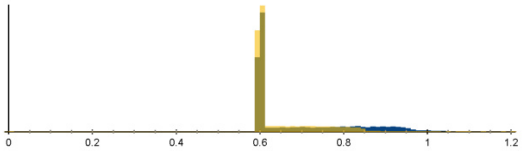

(b) Edge lengths distribution, target=0.6.

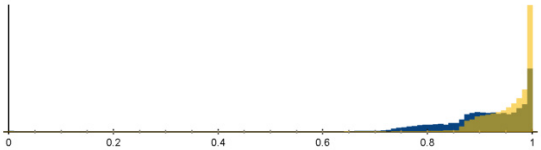

(c) Distribution of quality Q_t, target=1.0.

Figure 35: Histograms for remeshed *Screw*, with (blue) and without (yellow) feature detection, $\vartheta = 90°$.

d	ϑ	$\lvert\mathcal{V}\rvert$	$\lvert\mathcal{T}\rvert$	d_{avg}	$d_{\max}$	d_{RMS}	|feature segments|	|feature vertices|
0.6	—	13,411	26,842	0.0438	0.4605	138.1	—	—
0.6	90°	13,472	26,988	0.0190	0.3595	122.7	661,301	3,743

Table 23: Comparison of results achieved for *Screw*, with and without feature detection.

6.4 *Wrench*

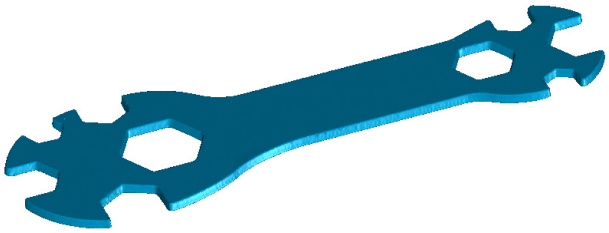

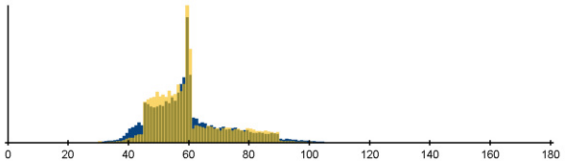

(a) Angle distribution, target=60°.

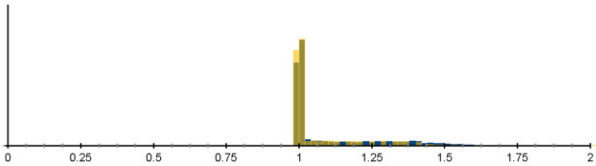

(b) Edge lengths distribution, target=1.0.

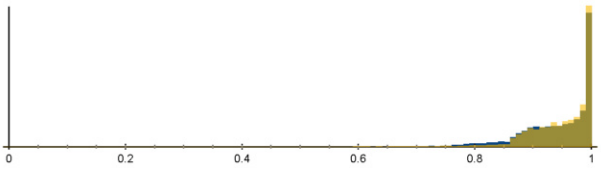

(c) Distribution of quality Q_t, target=1.0.

Figure 36: *Wrench*. Point cloud and histograms.

d	ϑ	$\lvert\mathcal{V}\rvert$	$\lvert\mathcal{T}\rvert$	d_{avg}	$d_{\max}$	d_{RMS}	|feature segments|	|feature vertices|
1.0	—	8,946	17,896	0.0360	0.6630	207.6	—	—
1.0	60°	8,871	17,746	0.0112	0.4353	189.7	583,665	1156

Table 24: Comparison of results achieved for *Wrench*, with and without feature detection, $\vartheta = 60°$.

6.5 *Xiao Jie Jie*

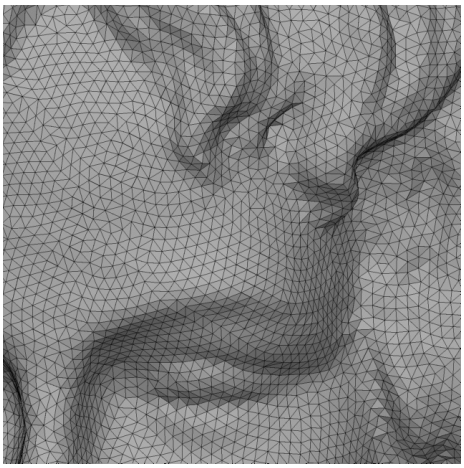

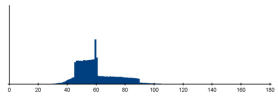

(a) Angle distribution, target=60°, $\vartheta = 40°$.

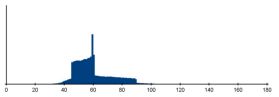

(d) Angle distribution, target=60°, $\vartheta = 50°$.

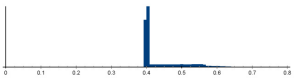

(b) Edge lengths distribution, target=0.4.

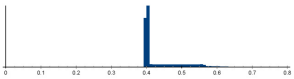

(e) Edge lengths distribution, target=0.4.

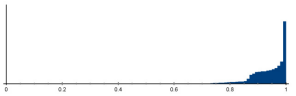

(c) Distribution of quality Q_t, target=1.0.

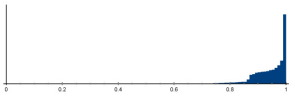

(f) Distribution of quality Q_t, target=1.0.

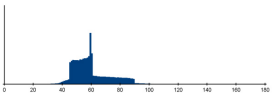

(g) Angle distribution, target=60°, $\vartheta = 60°$.

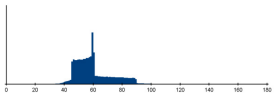

(j) Angle distribution, target=60°, $\vartheta = 70°$.

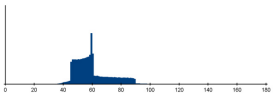

(m) Angle distribution, target=60°, $\vartheta = 80°$.

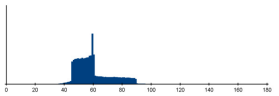

(p) Angle distribution, target=60°, $\vartheta = 90°$.

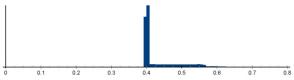

(h) Edge lengths distribution, target=0.4.

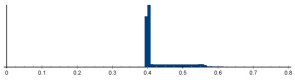

(k) Edge lengths distribution, target=0.4.

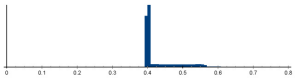

(n) Edge lengths distribution, target=0.4.

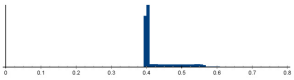

(q) Edge lengths distribution, target=0.4.

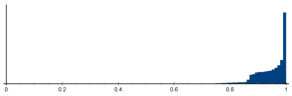

(i) Distribution of quality Q_t, target=1.0.

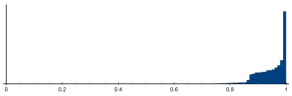

(l) Distribution of quality Q_t, target=1.0.

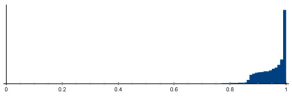

(o) Distribution of quality Q_t, target=1.0.

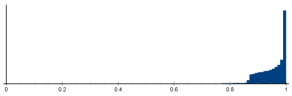

(r) Distribution of quality Q_t, target=1.0.

Figure 37: *Xiao Jie Jie*, remesh for $\vartheta = 70°$ and histograms for various thresholds.

d	ϑ	$\lvert\mathcal{V}\rvert$	$\lvert\mathcal{T}\rvert$	$\alpha_{\min}$	$\alpha_{\max}$	α_{avg}	α_{RMS}
0.4	40°	88,822	177,573	8.2213°	156.0215°	60°	22.3
0.4	50°	90,146	180,243	9.8948°	160.2103°	60°	21.2
0.4	60°	90,647	181,294	8.5513°	162.8973°	60°	20.8
0.4	70°	90,945	181,861	22.0826°	135.8347°	60°	20.5
0.4	80°	91,239	182,454	26.9329°	124.4023°	60°	20.2
0.4	90°	91,400	182,786	28.4372°	123.1255°	60°	20.1

$E_{\min}$	$E_{\max}$	E_{avg}	E_{RMS}	$Q_{\min}$	$Q_{\max}$	Q_{avg}	Q_{RMS}
0.3999	2.3119	0.4384	15.0	0.2407	1.0000	0.9420	6.1
0.3999	1.1101	0.4341	13.7	0.1993	1.0000	0.9474	5.6
0.3999	0.8867	0.4323	13.1	0.1723	1.0000	0.9494	5.3
0.3999	0.8564	0.4311	12.8	0.4441	1.0000	0.9508	5.1
0.3999	0.8406	0.4299	12.4	0.5571	1.0000	0.9524	4.9
0.3999	0.7903	0.4294	12.2	0.5696	1.0000	0.9530	4.8

Table 25: Comparison of results achieved for *Xiao Jie Jie*, with feature detection.

7 CAD Models for Feature Detection

7.1 *Flange*

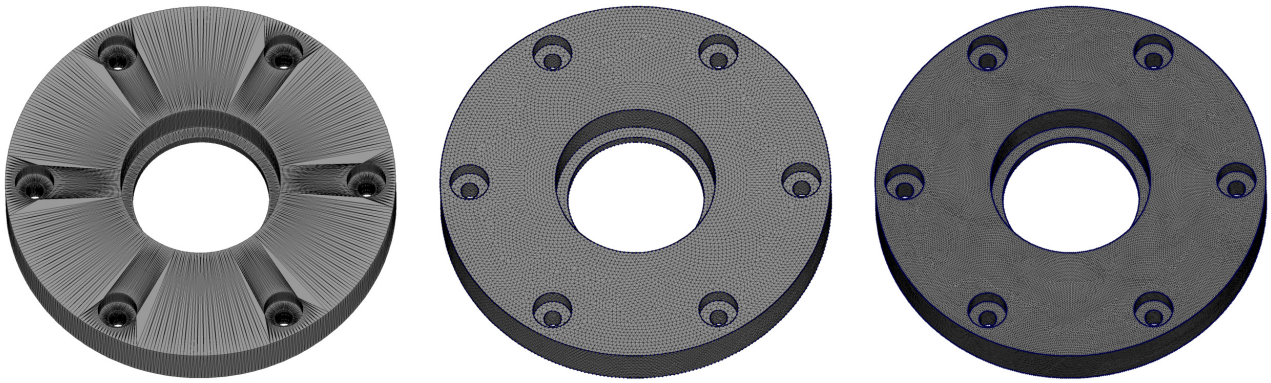

Figure 38: *Flange*. Left: CAD model. Middle: Model remeshed with features detected for $\vartheta = 80°$ and target edge length $d = 2.0$. Right: Model remeshed with features detected for $\vartheta = 80°$ and target edge length $d = 1.0$.

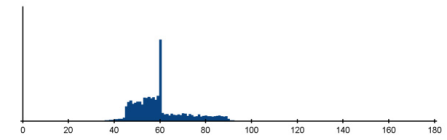

(a) Angle distribution, target=60°.

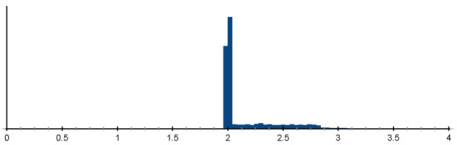

(b) Edge lengths distribution, target=2.0.

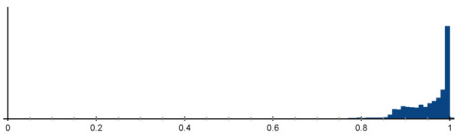

(c) Distribution of quality Q_t, target=1.0.

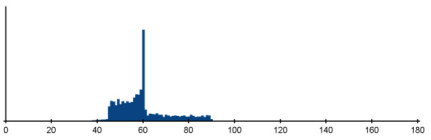

(d) Angle distribution, target=60°.

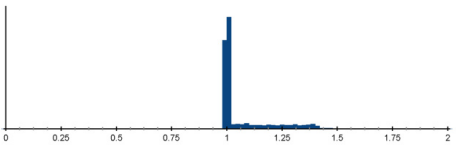

(e) Edge lengths distribution, target=1.0.

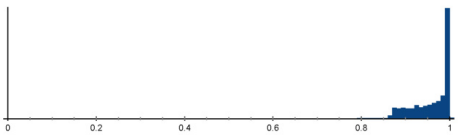

(f) Distribution of quality Q_t, target=1.0.

Figure 39: Histograms for remeshed *Flange*, $\vartheta = 80°$.

Algorithm	d	ϑ	$\lvert\mathcal{V}\rvert$	$\lvert\mathcal{T}\rvert$	$\alpha_{\min}$	$\alpha_{\max}$	α_{avg}	α_{RMS}
Meshlab	2.0	80°	23,627	47,378	14.8313°	122.7730°	60°	18.9
PMP	2.0	80°	28,432	56,888	15.9656°	137.0463°	60°	16.3
ours	2.0	80°	21,633	43,290	25.8987°	128.2024°	60°	19.7
Meshlab	1.0	80°	94,041	188,106	16.9999°	128.7068°	60°	17.8
PMP	1.0	80°	115,420	230,864	25.9868°	123.7041°	60°	17.2
ours	1.0	80°	87,643	175,310	25.5484°	128.9030°	60°	18.9

$E_{\min}$	$E_{\max}$	E_{avg}	E_{RMS}	$Q_{\min}$	$Q_{\max}$	Q_{avg}	Q_{RMS}
0.6472	3.7574	2.0475	14.2	0.4284	0.9999	0.9494	6.4
1.1490	3.3748	1.8591	12.1	0.3950	0.9999	0.9641	3.8
2.0	4.2169	2.1454	12.5	0.5198	1.0000	0.9546	5.2
0.3532	1.9557	1.0241	13.2	0.4545	0.9999	0.9562	5.1
0.5283	1.6284	0.9240	12.6	0.5626	0.9999	0.9601	3.8
1.0	2.0680	1.0645	11.8	0.5128	1.0000	0.9585	4.9

Table 26: Experimental results for *Flange*.

Algorithm	d	ϑ	$d_{\max}$	$\frac{d_{\max}}{d}$
Meshlab	1.0	80°	0.0590	0.0590
PMP	1.0	80°	0.0289	0.0289
ours	1.0	80°	0.0608	0.0608
Meshlab	2.0	80°	0.1781	0.0890
PMP	2.0	80°	0.1025	0.0512
ours	2.0	80°	0.3505	0.1752

Table 27: One-sided Hausdorff distance evaluated on the *Flange*.

7.2 *Body of Constant Width*

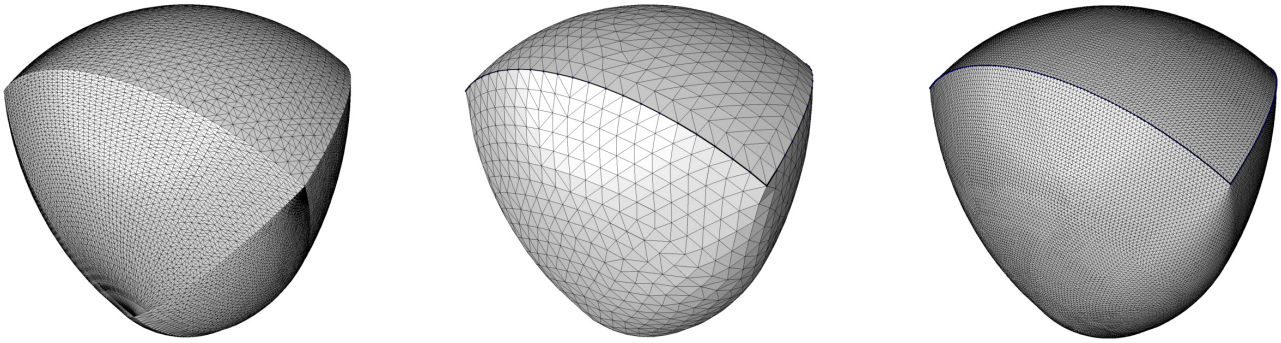

Figure 40: *Body of Constant Width.* Left: CAD model. Middle: Model remeshed with features detected for $\vartheta = 40°$ and target edge length $d = 0.1$. Right: Model remeshed with features detected for $\vartheta = 40°$ and target edge length $d = 0.02$.

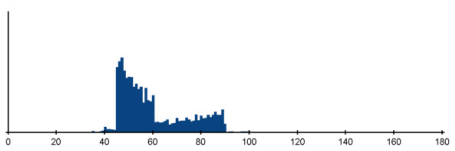

(a) Angle distribution, target=60°.

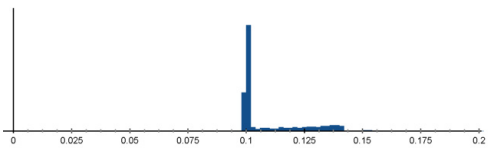

(b) Edge lengths distribution, target=0.1.

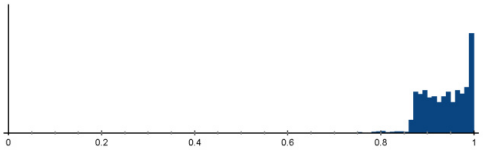

(c) Distribution of quality Q_t, target=1.0.

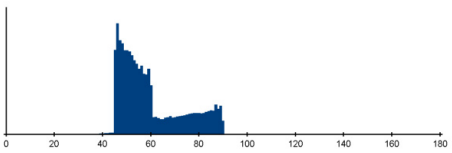

(d) Angle distribution, target=60°.

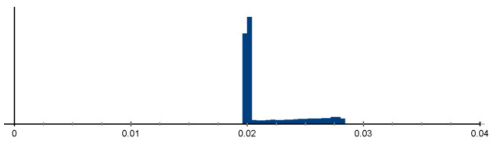

(e) Edge lengths distribution, target=0.02.

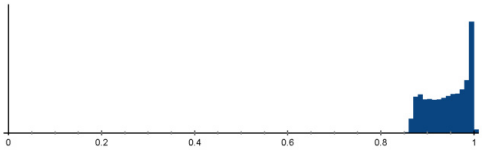

(f) Distribution of quality Q_t, target=1.0.

Figure 41: Histograms for remeshed *Body of Constant Width*, $\vartheta = 40°$.

Algorithm	|Iterations|	d	ϑ	$\lvert\mathcal{V}\rvert$	$\lvert\mathcal{T}\rvert$	$\alpha_{\min}$	$\alpha_{\max}$	α_{avg}	α_{RMS}
Meshlab	10	0.1	40°	1,374	2,744	26.8817°	109.9683°	60°	19.2
Meshlab	100	0.1	40°	1,303	2,602	27.1838°	106.8252°	60°	11.8
Meshlab	1,000	0.1	40°	1,281	2,558	32.7818°	106.4673°	60°	10.4
PMP	10	0.1	40°	1,600	3,196	29.4472°	114.4853°	60°	14.8
ours	1	0.1	40°	1,235	2,466	29.5060°	120.9878°	60°	23.2
Meshlab	10	0.02	40°	32,737	65,470	21.4255°	117.8555°	60°	15.9
Meshlab	100	0.02	40°	31,833	63,662	22.2400°	114.7592°	60°	10.6
Meshlab	1,000	0.02	40°	31,487	62,970	23.6324°	110.2686°	60°	8.2
PMP	10	0.02	40°	39,052	78,100	26.6413°	115.9396°	60°	15.4
ours	1	0.02	40°	31,277	62,550	30.1203°	115.0667°	60°	22.1

$E_{\min}$	$E_{\max}$	E_{avg}	E_{RMS}	$Q_{\min}$	$Q_{\max}$	Q_{avg}	Q_{RMS}
0.0561	0.1749	0.1021	13.4	0.6525	0.9999	0.9516	4.9
0.0512	0.1371	0.1036	10.5	0.6835	0.9999	0.9812	2.7
0.0566	0.1333	0.1043	10.1	0.7250	0.9999	0.9850	2.2
0.0603	0.1400	0.0940	11.5	0.6441	0.9999	0.9709	3.1
0.1	0.1884	0.1088	13.2	0.5904	1.0000	0.9380	13.2
0.0094	0.0366	0.0208	11.5	0.5774	0.9999	0.9645	4.4
0.0096	0.0335	0.0209	9.2	0.6041	0.9999	0.9840	2.5
0.0102	0.0304	0.0210	8.7	0.6223	0.9999	0.9903	1.9
0.0123	0.0328	0.0190	11.9	0.6155	0.9999	0.9678	3.5
0.02	0.0394	0.0215	12.3	0.6473	1.0000	0.9437	4.6

Table 28: Experimental results for *Body of Constant Width*.

Algorithm	|Iterations|	d	ϑ	$d_{\max}$	$\frac{d_{\max}}{d}$
Meshlab	10	0.02	40°	0.0046	0.2314
Meshlab	100	0.02	40°	0.0046	0.2315
PMP	10	0.02	40°	0.0038	0.1934
ours	1	0.02	40°	0.0017	0.0868
Meshlab	10	0.1	40°	0.0090	0.0904
Meshlab	100	0.1	40°	0.0108	0.1087
Meshlab	1000	0.1	40°	0.0135	0.1351
PMP	10	0.1	40°	0.0248	0.2480
ours	1	0.1	40°	0.0140	0.1404

Table 29: One-sided Hausdorff distance evaluated on the *Body of Constant Width*.

7.3 *Joint*

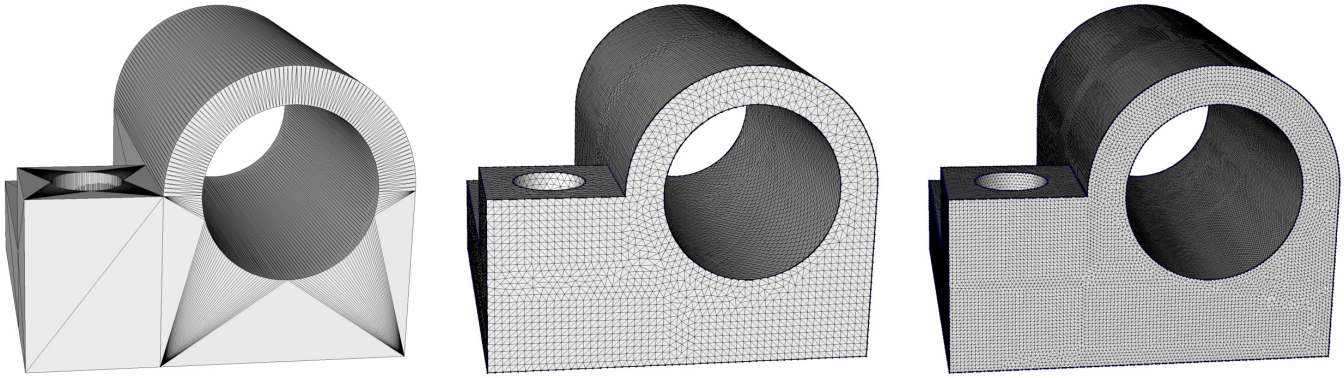

Figure 42: *Joint*. Left: CAD model. Middle: Model remeshed with features detected for $\vartheta = 80°$ and target edge length $d = 0.02$. Right: Model remeshed with features detected for $\vartheta = 80°$ and target edge length $d = 0.01$.

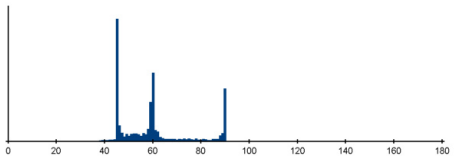

(a) Angle distribution, target=60°.

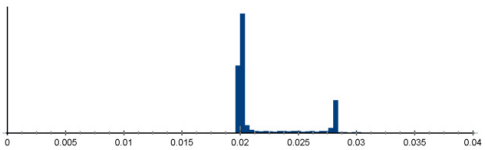

(b) Edge lengths distribution, target=0.02.

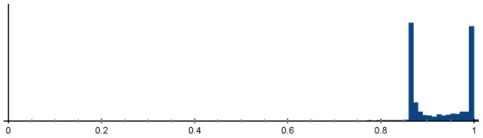

(c) Distribution of quality Q_t, target=1.0.

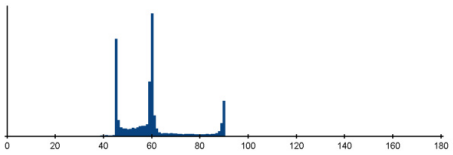

(d) Angle distribution, target=60°.

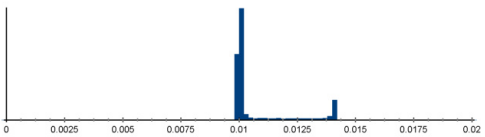

(e) Edge lengths distribution, target=0.01.

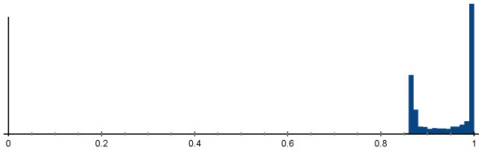

(f) Distribution of quality Q_t, target=1.0.

Figure 43: Histograms for remeshed *Joint*, $\vartheta = 80°$.

Algorithm	d	ϑ	$\lvert\mathcal{V}\rvert$	$\lvert\mathcal{T}\rvert$	$\alpha_{\min}$	$\alpha_{\max}$	α_{avg}	α_{RMS}
Meshlab	0.02	80°	19,743	39,490	17.5321°	120.6853°	60°	19.1
PMP	0.02	80°	23,046	46,096	21.4852°	129.5474°	60°	15.1
ours	0.02	80°	17,966	35,936	29.2933°	120.4075°	60°	25.7
Meshlab	0.01	80°	78,901	157,807	17.2320°	130.2468°	60°	19.8
PMP	0.01	80°	90,982	181,968	24.5734°	125.3222°	60°	15.4
ours	0.01	80°	73,474	146,952	24.0836°	131.8326°	60°	22.3

$E_{\min}$	$E_{\max}$	E_{avg}	E_{RMS}	$Q_{\min}$	$Q_{\max}$	Q_{avg}	Q_{RMS}
0.0085	0.0380	0.0204	14.1	0.4913	0.9999	0.9494	5.5
0.0115	0.0364	0.0188	11.8	0.4918	0.9999	0.9691	3.4
0.02	0.0416	0.0217	14.8	0.5960	1.0000	0.9272	6.6
0.0040	0.0193	0.0102	14.5	0.4847	0.9999	0.9458	5.8
0.0054	0.0165	0.0094	12.1	0.5476	0.9999	0.9681	3.2
0.01	0.0210	0.0106	13.3	0.4839	1.0000	0.9448	6.3

Table 30: Experimental results for *Joint*.

Algorithm	d	ϑ	$d_{\max}$	$\frac{d_{\max}}{d}$
Meshlab	0.01	80°	0.0003	0.0306
PMP	0.01	80°	0.0002	0.0206
ours	0.01	80°	0.0005	0.0543
Meshlab	0.02	80°	0.0008	0.0449
PMP	0.02	80°	0.0006	0.0308
ours	0.02	80°	0.0015	0.0780

Table 31: One-sided Hausdorff distance evaluated on the *Joint*.

7.4 *Oloid*

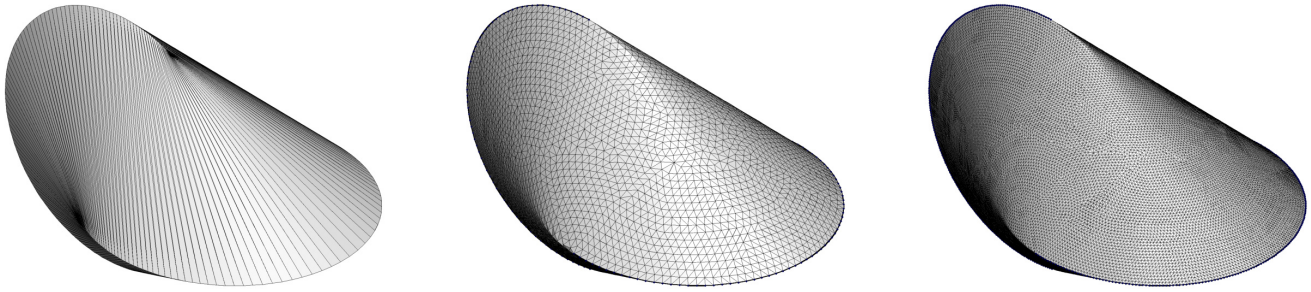

Figure 44: *Oloid*. Left: CAD model. Middle: Model remeshed with features detected for $\vartheta = 80°$ and target edge length $d = 0.05$. Right: Model remeshed with features detected for $\vartheta = 80°$ and target edge length $d = 0.02$.

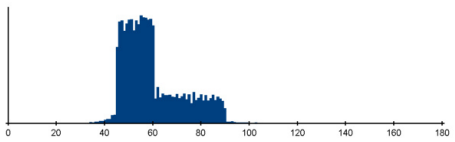

(a) Angle distribution, target=60°.

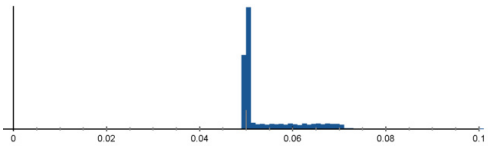

(b) Edge lengths distribution, target=0.05.

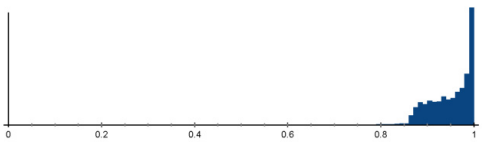

(c) Distribution of quality Q_t, target=1.0.

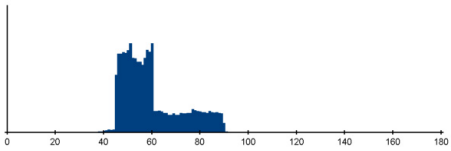

(d) Angle distribution, target=60°.

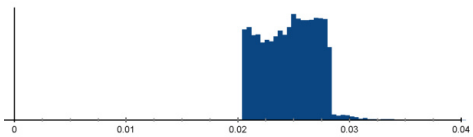

(e) Edge lengths distribution, target=0.02.

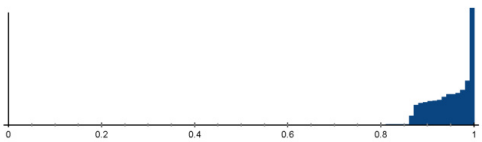

(f) Distribution of quality Q_t, target=1.0.

Figure 45: Histograms for remeshed *Oloid*, $\vartheta = 80°$.

Algorithm	|Iterations|	d	ϑ	$\lvert\mathcal{V}\rvert$	$\lvert\mathcal{T}\rvert$	$\alpha_{\min}$	$\alpha_{\max}$	α_{avg}	α_{RMS}
Meshlab	10	0.05	80°	5,980	11,956	0.0106°	179.9759°	60°	28.8
Meshlab	100	0.05	80°	5,355	10,706	30.1274°	106.6160°	60°	10.0
PMP	10	0.05	80°	6,709	13,414	25.3031°	112.5742°	60°	20.5
ours	1	0.05	80°	5,216	10,428	27.4950°	118.1905°	60°	20.7
Meshlab	10	0.02	80°	36,218	72,437	0.0151°	179.8044°	60°	21.4
Meshlab	100	0.02	80°	33,805	67,606	26.3402°	110.2882°	60°	9.9
PMP	10	0.02	80°	43,933	87,862	32.6637°	105.2212°	60°	16.8
ours	1	0.02	80°	32,787	65,570	28.5948°	122.8103°	60°	20.6

$E_{\min}$	$E_{\max}$	E_{avg}	E_{RMS}	$Q_{\min}$	$Q_{\max}$	Q_{avg}	Q_{RMS}
$4.9551E^{-4}$	0.0849	0.0494	21.0	$2.3800E^{-4}$	0.9999	0.9225	17.6
0.0264	0.0803	0.0521	9.8	0.6996	0.9999	0.9858	2.1
0.0296	0.0822	0.0474	13.3	0.6331	0.9999	0.9454	3.9
0.05	0.1038	0.0538	12.2	0.6164	1.0000	0.9501	4.7
$3.6697E^{-5}$	0.0376	0.0202	15.8	$4.5746E^{-4}$	0.9999	0.9455	9.4
0.0099	0.0324	0.0207	9.8	0.6440	0.9999	0.9862	1.9
0.0112	0.0308	0.0183	12.3	0.7291	0.9999	0.9624	3.4
0.02	0.0391	0.0214	11.8	0.5727	1.0000	0.9508	4.5

Table 32: Experimental results for *Oloid*.

Algorithm	|Iterations|	d	ϑ	$d_{\max}$	$\frac{d_{\max}}{d}$
Meshlab	10	0.02	80°	0.0072	0.3600
Meshlab	100	0.02	80°	0.0085	0.4293
PMP	10	0.02	80°	0.0154	0.7742
ours	1	0.02	80°	0.0071	0.35377
Meshlab	10	0.05	80°	0.0184	0.3695
Meshlab	100	0.05	80°	0.0205	0.4108
PMP	10	0.05	80°	0.0129	0.2590
ours	1	0.05	80°	0.0181	0.3628

Table 33: One-sided Hausdorff distance evaluated on the *Oloid*.

7.5 *Block*

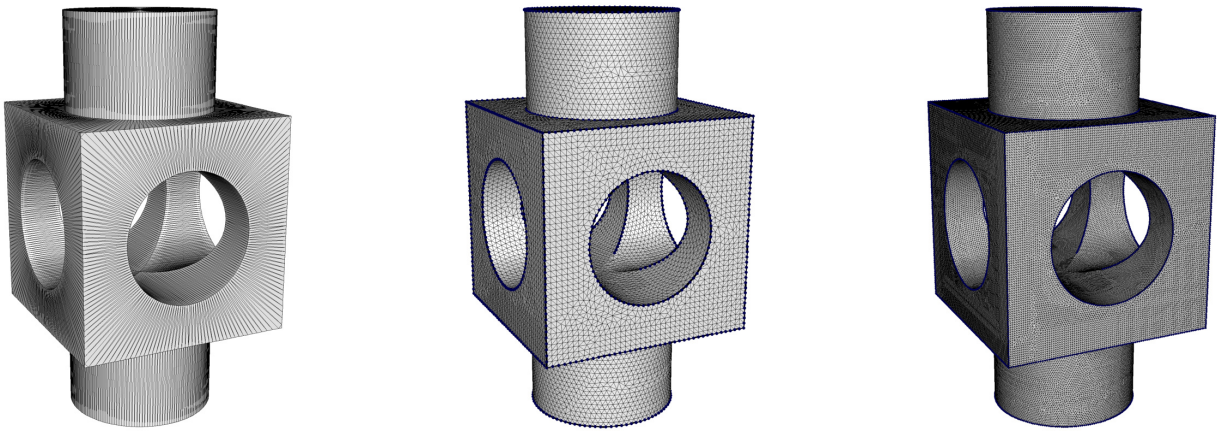

Figure 46: *Block*. Left: CAD model. Middle: Model remeshed with features detected for $\vartheta = 40°$ and target edge length $d = 0.5$. Right: Model remeshed with features detected for $\vartheta = 40°$ and target edge length $d = 0.2$.

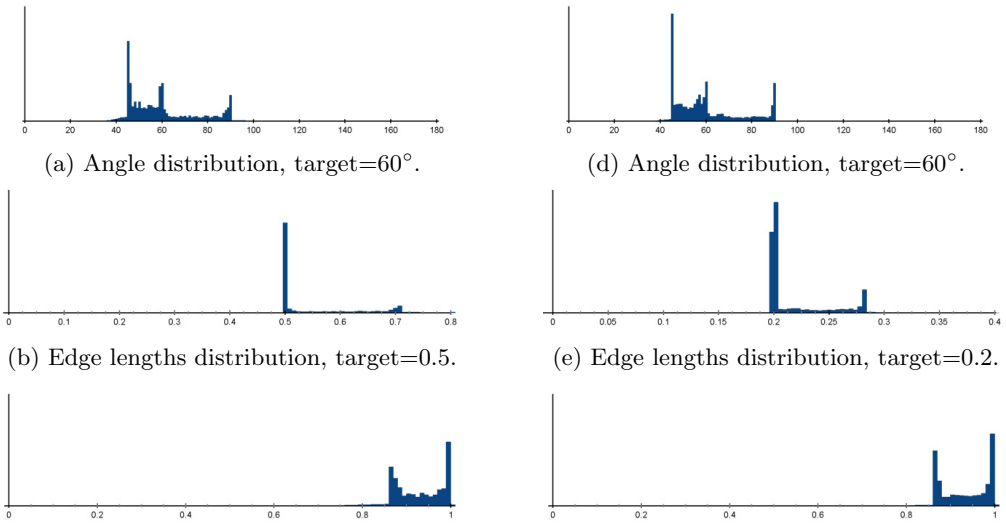

(a) Angle distribution, target=60°.

(b) Edge lengths distribution, target=0.5.

(c) Distribution of quality Q_t, target=1.0.

(d) Angle distribution, target=60°.

(e) Edge lengths distribution, target=0.2.

(f) Distribution of quality Q_t, target=1.0.

Figure 47: Histograms for remeshed *Block*, $\vartheta = 40°$.

Algorithm	d	ϑ	$\lvert\mathcal{V}\rvert$	$\lvert\mathcal{T}\rvert$	$\alpha_{\min}$	$\alpha_{\max}$	α_{avg}	α_{RMS}
Meshlab	0.5	40°	16,225	32,458	17.4712°	123.5228°	60°	17.6
PMP	0.5	40°	20,137	40,282	26.0368°	123.3726°	60°	17.3
ours	0.5	40°	14,963	29,934	25.0851°	120.2231°	60°	25.0
Meshlab	0.2	40°	101,174	202,356	0.0709°	179.8427°	60°	18.4
PMP	0.2	40°	125,027	250,062	24.9504°	123.8106°	60°	17.8
ours	0.2	40°	94,931	189,870	25.0891°	126.2225°	60°	24.5

$E_{\min}$	$E_{\max}$	E_{avg}	E_{RMS}	$Q_{\min}$	$Q_{\max}$	Q_{avg}	Q_{RMS}
0.2094	0.8994	0.5178	13.2	0.4619	0.9999	0.9568	5.0
0.3021	0.8054	0.4650	12.8	0.5663	0.9999	0.9590	3.9
0.4999	1.1090	0.5481	14.6	0.5978	1.0000	0.9294	6.1
0.0018	0.4033	0.2074	14.4	0.0015	0.9999	0.9541	5.6
0.1179	0.3243	0.1866	13.4	0.5622	0.9999	0.9589	3.6
0.1999	0.4488	0.2173	13.8	0.5393	1.0000	0.9331	5.9

Table 34: Experimental results for *Block*.

Algorithm	d	ϑ	$d_{\max}$	$\frac{d_{\max}}{d}$
Meshlab	0.2	40°	0.0298	0.1493
PMP	0.2	40°	0.0258	0.1293
ours	0.2	40°	0.0339	0.1698
Meshlab	0.5	40°	0.0828	0.1657
PMP	0.5	40°	0.0243	0.0486
ours	0.5	40°	0.0935	0.1871

Table 35: One-sided Hausdorff distance evaluated on the *Block*.

7.6 *Fandisk*

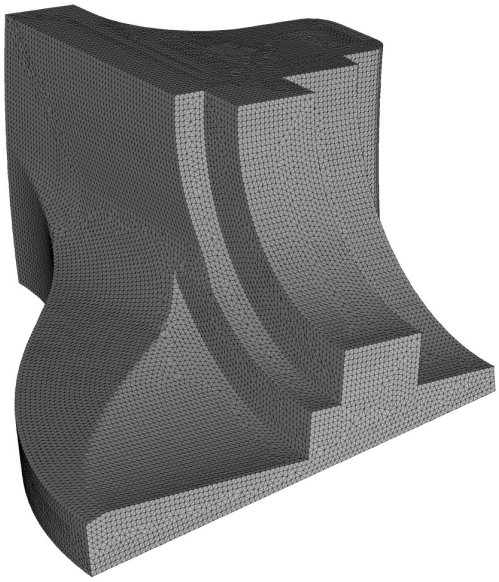

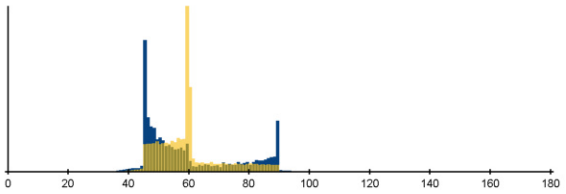

(a) Angle distribution, target=60°.

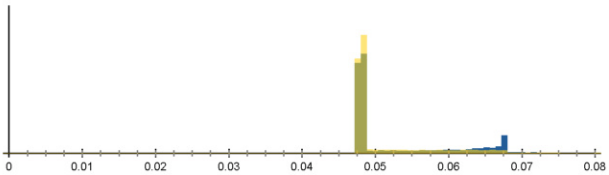

(b) Edge lengths distribution, target=0.048.

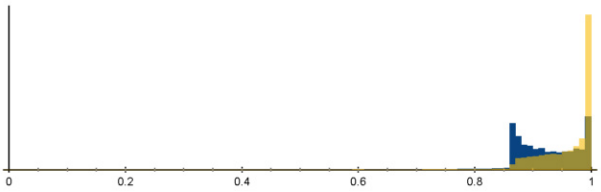

(c) Distribution of quality Q_t, target=1.0.

Figure 48: *Fandisk*. Remeshed model and histograms, $\vartheta = 60°$.

Algorithm	d	ϑ	$d_{\max}$	$\frac{d_{\max}}{d}$	Algorithm	d	ϑ	$d_{\max}$	$\frac{d_{\max}}{d}$
Meshlab	0.012	—	0.0111	0.9302	Meshlab	0.012	60°	0.0035	0.2929
PMP	0.012	—	0.0080	0.6721	PMP	0.012	60°	0.0027	0.2331
ours	0.012	—	0.0097	0.8147	ours	0.012	60°	0.0034	0.2835
Meshlab	0.024	—	0.0216	0.9039	Meshlab	0.024	60°	0.0061	0.2561
PMP	0.024	—	0.0180	0.7524	PMP	0.024	60°	0.0055	0.2302
ours	0.024	—	0.0184	0.7679	ours	0.024	60°	0.0072	0.2983
Meshlab	0.036	—	0.0318	0.8840	Meshlab	0.036	60°	0.0060	0.1690
PMP	0.036	—	0.0261	0.7252	PMP	0.036	60°	0.0088	0.2454
ours	0.036	—	0.0302	0.8376	ours	0.036	60°	0.0085	0.2367
Meshlab	0.048	—	0.0461	0.9618	Meshlab	0.048	60°	0.0115	0.2405
PMP	0.048	—	0.0334	0.6976	PMP	0.048	60°	0.0125	0.2612
ours	0.048	—	0.0337	0.7025	ours	0.048	60°	0.0134	0.2806

Table 36: One-sided Hausdorff distance evaluated on the *Fandisk*.

Algorithm	d	ϑ	$\lvert\mathcal{V}\rvert$	$\lvert\mathcal{T}\rvert$	$\alpha_{\min}$	$\alpha_{\max}$	α_{avg}	α_{RMS}
Meshlab	0.048	60°	28,316	56,628	18.3621°	123.6706°	60°	16.3
PMP	0.048	60°	36,135	72,266	18.2595°	125.1246°	60°	16.3
ours	0.048	60°	26,744	53,484	19.3842°	122.5733°	60°	25.8
Meshlab	0.048	—	28,124	56,244	21.0344°	121.2869°	60°	16.4
PMP	0.048	—	35,409	70,814	33.2363°	104.1949°	60°	15.4
ours	0.048	—	27,295	54,586	12.8282°	132.3435°	60°	19.0
Meshlab	0.036	60°	52,767	105,530	19.3825°	124.8048°	60°	16.9
PMP	0.036	60°	67,435	134,866	17.3648°	136.9920°	60°	15.8
ours	0.036	60°	47,114	95,424	27.8458°	123.7869°	60°	25.9
Meshlab	0.036	—	51,984	103,964	23.0220°	117.1838°	60°	16.3
PMP	0.036	—	66,275	132,546	25.1185°	119.1596°	60°	14.6
ours	0.036	—	48,788	97,572	21.96733°	121.1339°	60°	18.8
Meshlab	0.024	60°	115,999	231,994	18.3622°	128.1835°	60°	18.1
PMP	0.024	60°	139,962	279,920	16.9655°	126.8398°	60°	14.8
ours	0.024	60°	101,514	215,024	27.8458°	123.7869°	60°	25.9
Meshlab	0.024	—	115,464	230,924	18.6249°	128.1835°	60°	18.0
PMP	0.024	—	138,745	277,486	33.2062°	102.3007°	60°	14.4
ours	0.024	—	110,312	220,620	22.6942°	125.5307°	60°	18.7
Meshlab	0.012	60°	468,982	937,960	17.4867°	133.0335°	60°	18.9
PMP	0.012	60°	561,167	1,122,330	18.5464°	134.9632°	60°	14.5
ours	0.012	60°	431,506	863,008	19.3842°	125.0094°	60°	26.4
Meshlab	0.012	—	466,817	933,630	16.0072°	133.0326°	60°	18.8
PMP	0.012	—	558,622	1,117,240	33.4158°	101.9205°	60°	14.3
ours	0.012	—	443,351	886,698	19.4246°	134.0945°	60°	18.7

$E_{\min}$	$E_{\max}$	E_{avg}	E_{RMS}	$Q_{\min}$	$Q_{\max}$	Q_{avg}	Q_{RMS}
0.0162	0.0864	0.0502	11.8	0.5159	0.9999	0.9638	4.4
0.0162	0.0822	0.0445	12.7	0.5128	0.9999	0.9627	3.6
0.0208	0.1021	0.0528	14.4	0.5236	1.0000	0.9249	5.5
0.0243	0.0896	0.0500	12.1	0.5503	0.9999	0.9632	4.1
0.0278	0.0712	0.0446	12.4	0.7333	0.9999	0.9661	3.2
0.0447	0.1004	0.0512	11.4	0.4788	1.0000	0.9578	4.5
0.0176	0.0759	0.0368	12.0	0.5113	0.9999	0.9621	4.4
0.0207	0.0613	0.0325	12.6	0.4147	0.9999	0.9671	3.8
0.0198	0.0762	0.0395	14.3	0.5631	1.0000	0.9247	5.4
0.0180	0.0678	0.0368	16.3	0.5968	0.9999	0.9641	4.0
0.0206	0.0558	0.0326	12.0	0.5840	0.9999	0.9716	2.9
0.0359	0.0840	0.0383	11.3	0.5477	1.0000	0.9585	4.5
0.0081	0.0448	0.0249	12.7	0.4669	0.9999	0.9560	4.8
0.0081	0.0418	0.0225	12.3	0.4776	0.9999	0.9700	3.0
0.0158	0.0499	0.0263	26.3	0.5627	1.0000	0.9227	5.3
0.0116	0.0449	0.0248	12.7	0.4669	0.9999	0.9565	4.6
0.0140	0.0332	0.0225	12.1	0.7629	0.9999	0.9718	2.7
0.0239	0.0701	0.0255	11.2	0.5311	1.0000	0.9592	4.4
0.0040	0.0254	0.0124	18.9	0.4547	0.9999	0.9526	5.0
0.0040	0.0218	0.0112	12.3	0.4462	0.9999	0.9713	2.9
0.0044	0.0257	0.0131	14.2	0.5392	1.0000	0.9221	5.3
0.0038	0.0250	0.0124	12.9	0.4164	0.9999	0.9531	4.9
0.0069	0.0173	0.1125	12.2	0.7625	0.9999	0.9720	2.8
0.0119	0.0272	0.0127	11.1	0.4470	1.0000	0.9592	4.4

Table 37: Experimental results for *Fandisk*, displaying edges shorter than target edge length d. Meshlab and PMP were run with 10 iterations each, which corresponds to the standard setting in both.

7.7 *Cube*

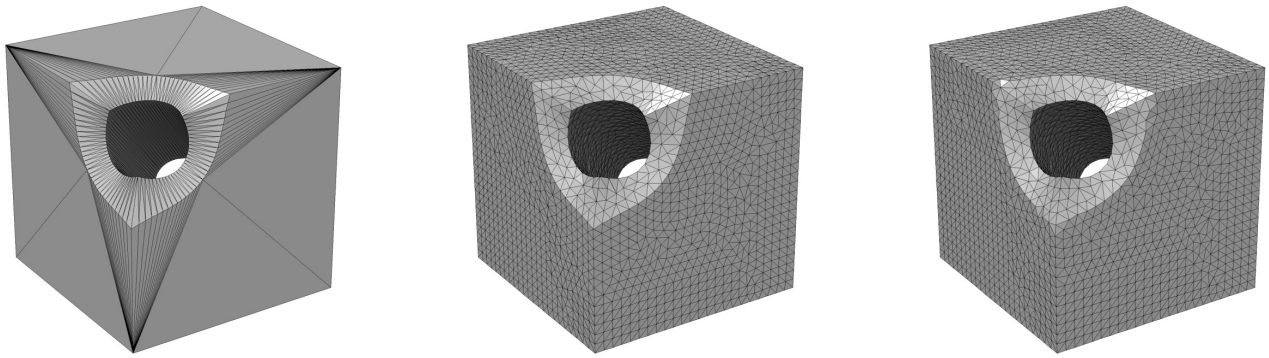

Figure 49: *Cube*. Left: CAD model. Middle: Model remeshed with features detected for $\vartheta = 24°$ and target edge length $d = 0.1$. Right: Model remeshed with features detected for $\vartheta = 40°$ and target edge length $d = 0.1$.

Algorithm	d	ϑ	$\lvert\mathcal{V}\rvert$	$\lvert\mathcal{T}\rvert$	$\alpha_{\min}$	$\alpha_{\max}$	α_{avg}	α_{RMS}
Meshlab	0.1	24°	4,185	8,370	14.8334°	127.2719°	60°	18.9
PMP	0.1	24°	5,480	10,960	20.9229°	135.1919°	60°	18.4
ours	0.1	24°	3,796	7,592	28.5518°	115.6221°	60°	26.6
Meshlab	0.1	40°	3,778	7,556	28.7024°	120.7229°	60°	27.4
PMP	0.1	40°	5,470	10,940	18.4349°	135.0000°	60°	17.9
ours	0.1	40°	3,778	7,556	28.7024°	120.7229°	60°	27.4
Meshlab	0.1	—	4,159	8,318	6.5643°	139.1714°	60°	21.7
PMP	0.1	—	5,302	10,604	35.9060°	98.8441°	60°	14.9
ours	0.1	—	3,896	7,792	31.0974°	115.6319°	60°	18.9
Meshlab	0.04	24°	26,889	53,778	2.2081°	122.0278°	60°	17.1
PMP	0.04	24°	33,817	67,634	26.3548°	119.3944°	60°	16.6
ours	0.04	24°	24,331	48,662	25.2122°	129.5755°	60°	25.1
Meshlab	0.04	40°	25,889	53,778	23.2081°	122.0278°	60°	17.1
PMP	0.04	40°	33,781	67,562	26.2303°	119.5088°	60°	16.6
ours	0.04	40°	24,667	49,334	27.2235°	124.2618°	60°	22.1
Meshlab	0.04	—	27,113	54,226	4.2034°	142.9207°	60°	18.5
PMP	0.04	—	33,422	66,844	32.2670°	107.9337°	60°	16.0
ours	0.04	—	24,735	49,470	30.4114°	116.7102°	60°	18.9

$E_{\min}$	$E_{\max}$	E_{avg}	E_{RMS}	$Q_{\min}$	$Q_{\max}$	Q_{avg}	Q_{RMS}
0.0370	0.1875	0.1037	14.5	0.4166	0.9999	0.9511	5.9
0.0553	0.1767	0.0907	13.1	0.4478	0.9999	0.9566	4.9
0.1	0.2068	0.1110	15.2	0.6420	1.0000	0.9202	5.9
0.0999	0.2046	0.1114	15.5	0.5929	0.9999	0.9155	5.9
0.0546	0.1759	0.0907	12.9	0.4330	0.9999	0.9587	4.8
0.1	0.2046	0.1114	15.5	0.6419	1.0000	0.9155	11.8
0.0125	0.1698	0.1026	17.4	0.1953	0.9999	0.9340	11.3
0.0604	0.1314	0.0907	11.7	0.7942	0.9999	0.9694	2.9
0.1	0.1927	0.1066	11.8	0.6419	1.0000	0.9582	4.8
0.0189	0.0805	0.0408	12.8	0.5625	0.9999	0.9600	4.5
0.0237	0.0670	0.0364	12.2	0.5923	0.9999	0.9636	3.5
0.04	0.0809	0.0436	14.1	0.5062	1.0000	0.9295	5.8
0.0027	0.0736	0.0404	14.5	0.1264	0.9999	0.9525	7.3
0.0237	0.0670	0.0364	12.1	0.5923	0.9999	0.9637	3.5
0.04	0.0855	0.0431	13.1	0.5585	1.0000	0.9445	5.6
0.0027	0.0736	0.0404	14.5	0.1264	0.9999	0.9525	7.3
0.0238	0.0587	0.0364	11.8	0.7125	0.9999	0.9663	3.1
0.04	0.0789	0.0426	11.3	0.6316	1.0000	0.9584	4.5

Table 38: Experimental results for *Cube*.

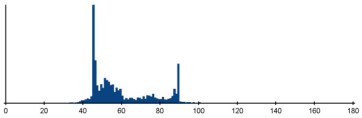

(a) Angle distribution, target=60°.

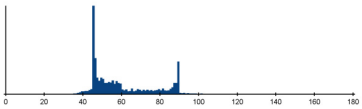

(d) Angle distribution, target=60°.

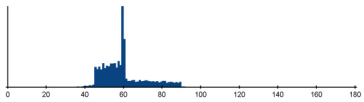

(g) Angle distribution.

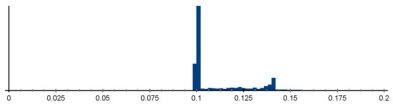

(b) Edge lengths distribution, target=0.1.

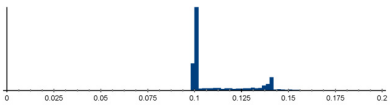

(e) Edge lengths distribution, target=0.1.

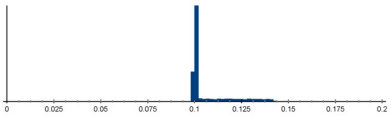

(h) Edge lengths distribution, target=0.1.

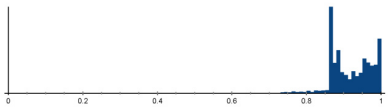

(c) Distribution of quality Q_t, target=1.0.

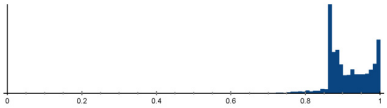

(f) Distribution of quality Q_t, target=1.0.

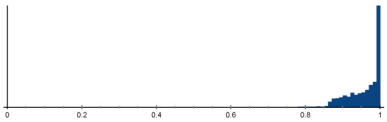

(i) Distribution of quality Q_t, target=1.0.

Figure 50: Histograms for remeshed *Cube* for $d = 0.1$. From left to right: $\vartheta = 24°$, $\vartheta = 40°$, no feature detection.

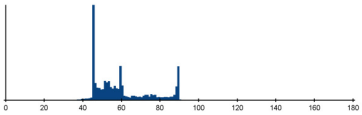

(a) Angle distribution, target=60°.

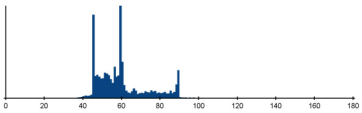

(d) Angle distribution, target=60°.

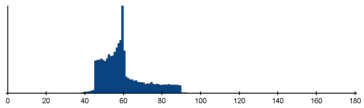

(g) Angle distribution.

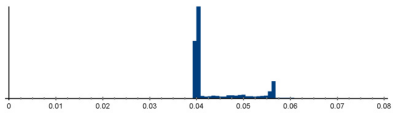

(b) Edge lengths distribution, target=0.04.

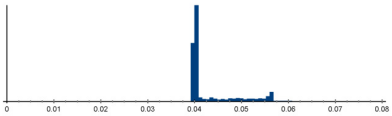

(e) Edge lengths distribution, target=0.04.

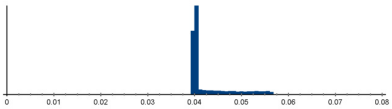

(h) Edge lengths distribution, target=0.04.

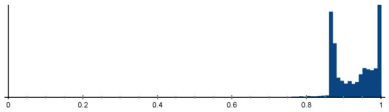

(c) Distribution of quality Q_t, target=1.0.

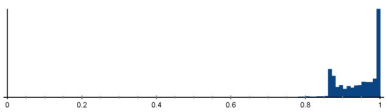

(f) Distribution of quality Q_t, target=1.0.

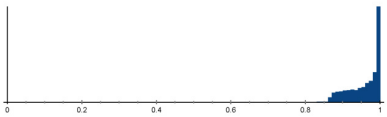

(i) Distribution of quality Q_t, target=1.0.

Figure 51: Histograms for remeshed *Cube* for $d = 0.04$. From left to right: $\vartheta = 24°$, $\vartheta = 40°$, no feature detection.

Algorithm	d	ϑ	$d_{\max}$	$\frac{d_{\max}}{d}$	Algorithm	d	ϑ	$d_{\max}$	$\frac{d_{\max}}{d}$
Meshlab	0.04	—	0.0347	0.8687	Meshlab	0.1	—	0.0808	0.8082
PMP	0.04	—	0.0334	0.8353	PMP	0.1	—	0.2781	0.6623
ours	0.04	—	0.0324	0.8122	ours	0.1	—	0.0776	0.7765
Meshlab	0.04	24°	0.0043	0.1078	Meshlab	0.1	24°	0.0062	0.0620
PMP	0.04	24°	0.0038	0.0951	PMP	0.1	24°	0.0061	0.0614
ours	0.04	24°	0.0042	0.1059	ours	0.1	24°	0.0084	0.0843
Meshlab	0.04	40°	0.0043	0.1033	Meshlab	0.1	40°	0.0190	0.1908
PMP	0.04	40°	0.0065	0.1637	PMP	0.1	40°	0.0196	0.1961
ours	0.04	40°	0.0097	0.2427	ours	0.1	40°	0.0213	0.2134

Table 39: One-sided Hausdorff distance evaluated on the *Cube*.

7.8 *Boat*

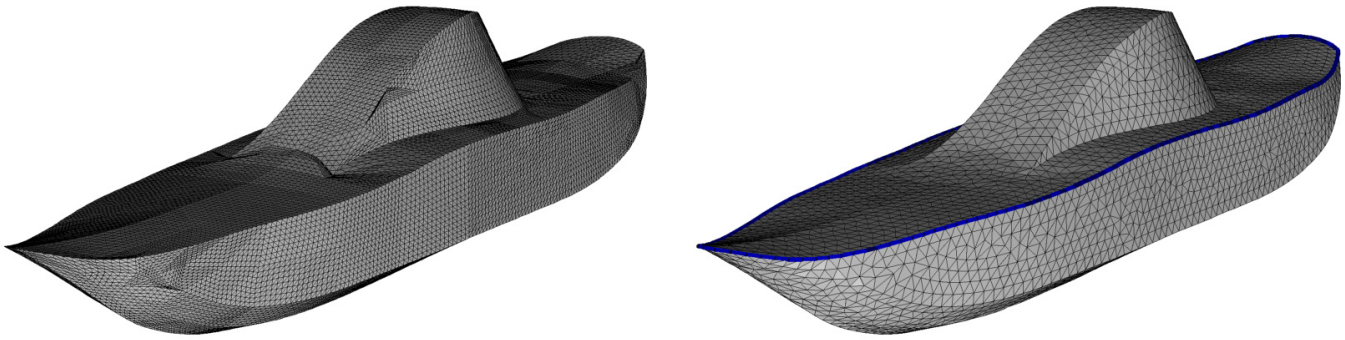

Figure 52: *Boat*. Left: CAD model. Right: *Boat* model remeshed after splitting along closing features.

Algorithm	d	ϑ	$\lvert\mathcal{V}\rvert$	$\lvert\mathcal{T}\rvert$	$\alpha_{\min}$	$\alpha_{\max}$	α_{avg}	α_{RMS}
Meshlab	0.1	30°	4,394	8,784	8.6603°	157.4566°	60°	16.7
PMP	0.1	30°	5,388	10,772	11.8547°	130.3723°	60°	15.2
ours	0.1	30°	4,051	8,098	4.2360°	130.0883°	60°	20.6

$E_{\min}$	$E_{\max}$	E_{avg}	E_{RMS}	$Q_{\min}$	$Q_{\max}$	Q_{avg}	Q_{RMS}
0.0167	0.1782	0.1027	12.9	0.2164	0.9999	0.9617	5.4
0.0223	0.1672	0.092	12.1	0.3474	0.9999	0.9694	4.1
0.0078	0.1976	0.1079	13.3	0.1274	1.0000	0.9500	6.2

Table 40: Experimental results for *Boat*.

Algorithm	d	ϑ	$d_{\max}$	$\frac{d_{\max}}{d}$
Meshlab	0.1	30°	0.0158	0.1582
PMP	0.1	30°	0.0143	0.1435
ours	0.1	30°	0.0156	0.1566

Table 41: One-sided Hausdorff distance evaluated on the *Boat*.

7.9 *Kitten*

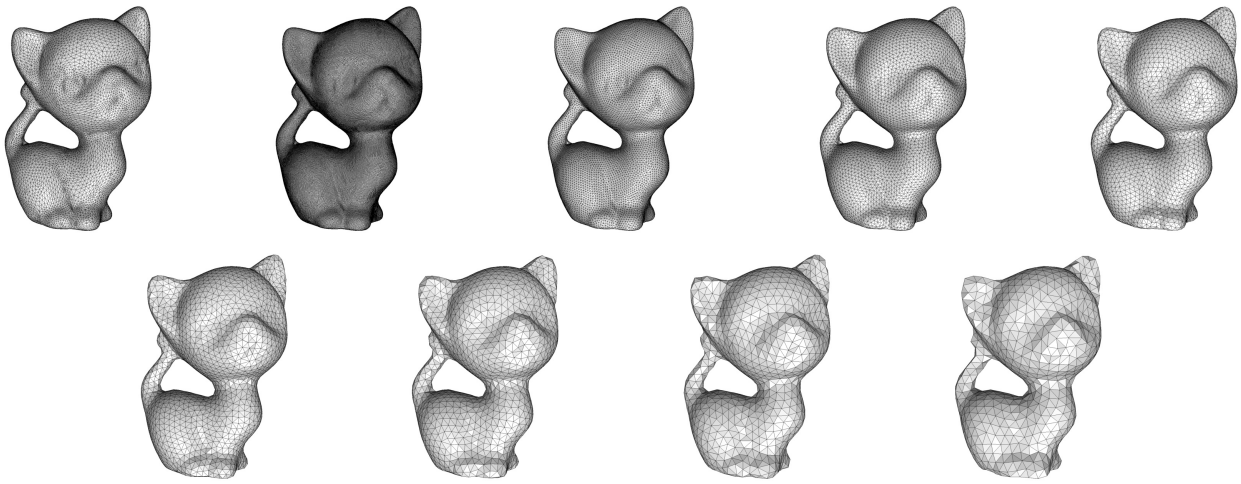

Figure 53: *Kitten*. Upper row, from left to right: input model, followed by results achieved for target edge length $d \in \{0.01, 0.02, 0.03, 0.04\}$. Lower row, from left to right: results achieved for target edge length $d \in \{0.05, 0.06, 0.07, 0.08\}$.

	d	$\lvert\mathcal{V}\rvert$	$\lvert\mathcal{T}\rvert$	$\alpha_{\min}$	$\alpha_{\max}$	α_{avg}	α_{RMS}
input	—	10,000	20,000	7.6919°	153.3379°	60°	35.9
remesh	0.01	70,981	141,962	28.1880°	122.9065°	60°	19.3
remesh	0.02	17,673	35,346	30.2108°	112.2197°	60°	19.5
remesh	0.03	7,837	15,674	28.3165°	115.9218°	60°	19.6
remesh	0.04	4,387	8,774	30.1886°	112.2698°	60°	19.8
remesh	0.05	2,797	5,594	30.3553°	110.9096°	60°	19.8
remesh	0.06	1,933	3,866	32.7483°	108.4652°	60°	20.3
remesh	0.07	1,417	2,834	31.2655°	112.4897°	60°	19.6
remesh	0.08	1,080	2,160	32.0148°	109.0594°	60°	20.0

$E_{\min}$	$E_{\max}$	E_{avg}	E_{RMS}	$Q_{\min}$	$Q_{\max}$	Q_{avg}	Q_{RMS}
0.0039	0.1119	0.0287	38.2	0.2296	0.9999	0.8438	16.4
0.01	0.0210	0.0106	11.3	0.5717	1.0000	0.9566	4.4
0.02	0.0391	0.0213	11.5	0.6742	1.0000	0.9558	4.5
0.03	0.0613	0.0320	11.8	0.6391	1.0000	0.9552	4.7
0.04	0.0782	0.0428	12.1	0.6737	1.0000	0.9542	4.8
0.05	0.9594	0.0536	12.1	0.6864	1.0000	0.9542	4.8
0.06	0.1106	0.0644	12.3	0.7091	1.0000	0.9520	4.9
0.07	0.1304	0.0751	12.1	0.6716	1.0000	0.9549	4.7
0.08	0.1485	0.0859	12.4	0.7036	1.0000	0.9532	4.9

Table 42: Experimental results for remeshing *Kitten*.

Algorithm	d	$d_{\max}$	$\frac{d_{\max}}{d}$	Algorithm	d	$d_{\max}$	$\frac{d_{\max}}{d}$
ours	0.01	0.0054	0.5406	ours	0.06	0.0319	0.5328
ours	0.02	0.0082	0.4145	ours	0.08	0.0410	0.5135
ours	0.04	0.0250	0.6266				

Table 43: One-sided Hausdorff distance evaluated on the *Kitten*.

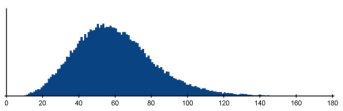

Angle distribution.

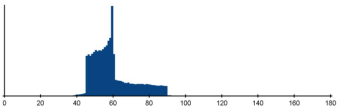

Angle distribution.

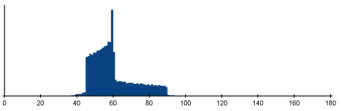

Angle distribution.

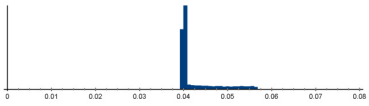

Edge lengths distribution.

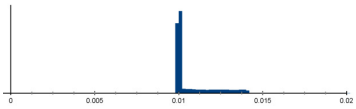

Edge lengths distribution.

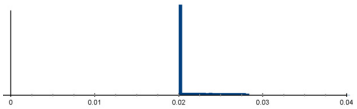

Edge lengths distribution.

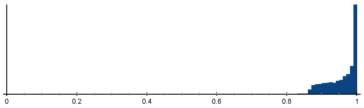

Distribution of quality Q_t.

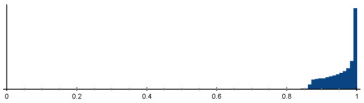

Distribution of quality Q_t.

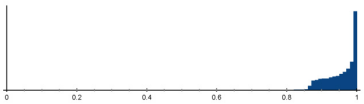

Distribution of quality Q_t.

Histogram of input.

Histograms for $d = 0.01$.

Histograms for $d = 0.02$.

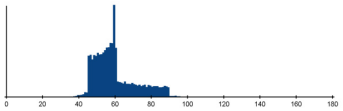

Angle distribution.

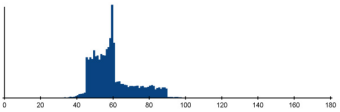

Angle distribution.

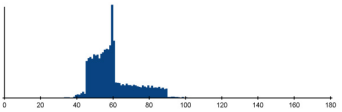

Angle distribution.

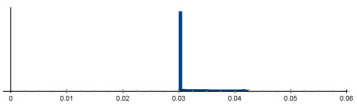

Edge lengths distribution.

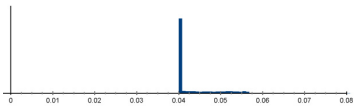

Edge lengths distribution.

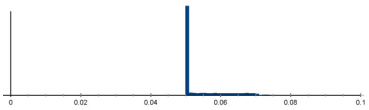

Edge lengths distribution.

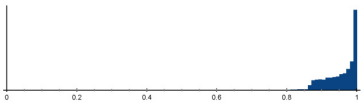

Distribution of quality Q_t.

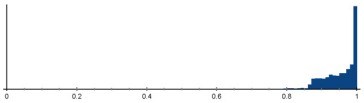

Distribution of quality Q_t.

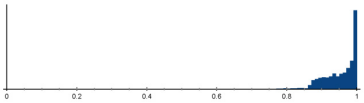

Distribution of quality Q_t.

Histograms for $d = 0.03$.

Histograms for $d = 0.04$.

Histograms for $d = 0.05$.

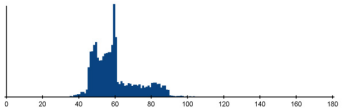

Angle distribution.

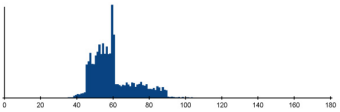

Angle distribution.

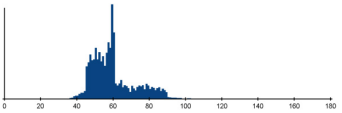

Angle distribution.

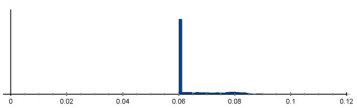

Edge lengths distribution.

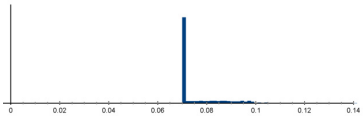

Edge lengths distribution.

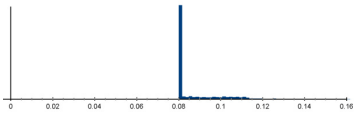

Edge lengths distribution.

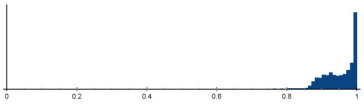

Distribution of quality Q_t.

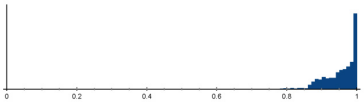

Distribution of quality Q_t.

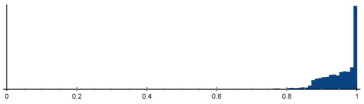

Distribution of quality Q_t.

Histograms for $d = 0.06$.

Histograms for $d = 0.07$.

Histograms for $d = 0.08$.

Figure 54: Histograms for *Kitten* model with various target edge lengths and without feature detection.